UNIVERSIDADE BEIRA INTERIOR

Physical and Chemical Parameters Screening for Co-Crystallization of rS -COMT-entacapone

Pedro Daniel de Jesus Conde Fernandes

Dissertação para obtenção do Grau de Mestre em

Biotecnologia

(2ºciclo de estudos)

Orientadora: Prof. Doutora Filipa Juliana Fernandes Castro

Coorientador: Prof. Doutor Luís António Paulino Passarinha

Janeiro 2023

Declaração de Integridade

Eu, Pedro Daniel de Jesus Conde Fernandes, que abaixo assino, estudante com o número de inscrição M11125 de Biotecnologia da Faculdade de Ciências, declaro ter desenvolvido o presente trabalho e elaborado o presente texto em total consonância com o **Código de Integridades da Universidade da Beira Interior**.

Mais concretamente afirmo não ter incorrido em qualquer das variedades de Fraude Académica, e que aqui declaro conhecer, que em particular atendi à exigida referenciação de frases, extratos, imagens e outras formas de trabalho intelectual, e assumindo assim na íntegra as responsabilidades da autoria.

Universidade da Beira Interior, Covilhã 31/ 01 / 2023

Acknowledgments

Primeiramente, queria agradecer aos meus Pais dignos de letra grande, que estão cá para o bem e para o mal, sem eles nada disto era possível e à melhor pessoa da minha vida, uma Mulher que tenho um enorme orgulho e que acreditou sempre em mim, a minha irmã. Obrigado pela educação, pela motivação, pelos "carolos" e por tornarem tudo isto possível, nunca se esqueçam do que valem para mim.

Aos meus amigos, vocês sabem quem são, obrigado por me terem acompanhado nesta jornada, por fazerem parte das histórias e ao "Miguxamuxo", um brinde especial a vocês.

Quero deixar um agradecimento especial à Professora Filipa pela seu suporte e ajuda incondicional e ao Professor Luís, um obrigado por tudo o que me ensinou, espero ter estado à altura do desafio.

Que tenhamos sempre saúde para as histórias nunca acabarem.

Nunca será um Adeus, para ti Covilhã, será sempre um Até já.

Bem Haja!

Resumo alargado

A catecol-*O*-metiltransferase (COMT, EC 2.2.1.6) é a enzima responsável pela *O*-metilação de substratos como as catecolaminas e os estrogénios com estrutura tipicamente catecólica. Considerando as suas funções fisiológicas e a existência de polimorfismos intrínsecos, vários estudos associam a COMT com a patogénese de inúmeras desordens neurológicas, especialmente com a Doença de Parkinson (DP) e também com doenças cardiovasculares e neoplasias hormônio-dependentes, como o cancro de mama. Devido à importância que a COMT tem no metabolismo humano, a enzima tornou-se nas últimas décadas num relevante alvo terapêutico. Desta forma, a proteína foi estudada e foi descoberto que um único gene codifica duas isoformas da proteína, uma forma solúvel (SCOMT) e uma forma ligada à membrana (MBCOMT). Especificamente, a SCOMT participa na inativação e desintoxicação de moléculas catecólicas biologicamente ativas ou tóxicas e os seus metabolitos hidroxilados, como 2-hidroxiestradiol, 2-hidroxiestrona, 4-hidroxiestradiol e 4-hidroxiestrona. O desenvolvimento de estratégias para a obtenção de rendimentos elevados de frações contendo a enzima biologicamente ativa, estável e pura permanece um objetivo essencial, aplicando-se a um nível de proteínas terapêuticas ou à realização de estudos estruturais. Uma vez que a COMT perde rapidamente a sua atividade biológica durante o processo de recuperação e armazenamento, é considerada uma enzima altamente instável e termolábil. Tipicamente, a COMT pode ser estabilizada através de moléculas específicas capazes de aumentar a sua estabilidade termodinâmica evitando assim a sua desnaturação e perda de atividade. Deste modo, as soluções estabilizadoras que foram empregues incluíram compostos que são agentes redutores como a cisteína, que geralmente, desempenha um papel na formação de ligações dissulfeto intramoleculares e intermoleculares, açúcares que protegem as proteínas da desnaturação *in vivo* e também foram descritos como promotores do *folding* e *refolding* de proteínas e ainda o glicerol que tem sido aplicado para termoestabilização de enzimas. Nos últimos anos, os líquidos iónicos (ILs) demonstraram uma capacidade única de preservar a estabilidade e a conformação de proteínas e prevenir a sua agregação, devido às diversas combinações de iões que lhes conferem diferentes propriedades físico-químicas. Depois de garantir as condições ótimas de atividade, estabilidade e pureza da proteína, a realização de estudos estruturais é o próximo passo. Nestes estudos são realizados ensaios de cristalização com o objetivo de formar um cristal, em que as moléculas de proteínas estão organizadas de forma regular e ordenada, para obter informação sobre a sua estrutura tridimensional.

Neste trabalho, avaliámos o efeito da interação dos líquidos iónicos na atividade enzimática da SCOMT e investigámos as condições de cristalização de frações purificadas da mesma. Primeiramente, estudámos a influência de dois líquidos iônicos, di-hidrogenofosfato de

colina ([Ch][DHP]) e o cloreto de 1-butil-3-metilimidazólio ([C_4mim]Cl), no lisado de SCOMT por 12 horas aplicando uma temperatura de armazenamento de 4 ºC ou -80 ºC e se os líquidos iónicos aumentariam a estabilidade da proteína, avaliando-se a sua atividade específica. Um maior efeito estabilizador potencial foi obtido usando [C_4mim]Cl (10 mM) a 4 ºC, com uma recuperação de atividade de cerca 350% durante 12 horas. Em seguida, foram realizados testes de cristalização de frações purificadas de SCOMT, usando os métodos de difusão de vapor (Hanging Drop) e contra difusão, onde foram avaliados vários fatores, nomeadamente, a temperatura (4 ºC e 20 ºC), a concentração e composição da solução do agente precipitante (HEPES, pH=7.5, metil-2,4-pentanediol e Caps, pH 10.5, Li_2SO_4, NaH_2PO_4/ K_2HPO_4) e a influência de S-adenosil-L-metionina (SAM) e 3,5-dinitrocatechol (DNC), um cofator e um inibidor da COMT, respetivamente. Ao avaliar os vários fatores, conseguimos concluir que se obtiveram melhores resultados a uma temperatura de 20 ºC, que corresponde a uma solução de agente precipitante composta por Caps, pH 10.5, Li_2SO_4, NaH_2PO_4/ K_2HPO_4 e que, a técnica de difusão a vapor mostrou resultados mais promissores. Além disso, foi observado ao longo dos ensaios uma elevada concentração de precipitados, na sua maioria DNC e, na minoria, sais presentes na solução do agente precipitante. Num último passo foram classificados os resultados obtidos, nomeadamente, distinguir os cristais de proteína dos cristais de sal, mas devido ao seu tamanho reduzido, a identificação por raio-X não foi possível, uma vez que os cristais precisam de ter uma dimensão de 0.1 mm de acordo com as caraterísticas do equipamento que tínhamos em disposição no Instituto de Investigação e Inovação em Saúde do Porto (i3S) . Deste modo, como alternativa, foram realizados testes como a absorção de corantes (Azul de Timol e Azul de Coomassie), que permite colorir apenas os cristais de proteína, e o Crush Test, que permite diferenciar os cristais de sal dos cristais de proteína de acordo com a facilidade que um cristal de proteína se desintegra ao aplicar uma força. Estes testes demonstraram resultados inconclusivos, uma vez que, devido à reduzida dimensão dos cristais, não foi possível identificar com certeza a natureza deles.

Palavras-Chave

Cristalização; Estabilidade; Inibidores; Líquidos Iónicos; SCOMT.

Abstract

Catechol-*O*-methyltransferase (COMT, EC 2.2.1.6) is the enzyme responsible for the *O*-methylation of substrates such as catecholamines and estrogens with a typically catechollic structure. Commonly, COMT can be stabilized through specific molecules capable of increasing its thermodynamic stability, thus preventing its denaturation and loss of activity. After ensuring optimal conditions for protein activity, stability, and purity, carrying out structural studies is the next step. In these studies, crystallization tests are carried out with the aim of forming a crystal, in which the protein molecules are organized in a regular and orderly manner, to obtain information about their three-dimensional structure.

In this work, we evaluated the effect of the interaction of ionic liquids on the enzymatic activity of SCOMT and investigated the crystallization conditions of purified SCOMT fractions. Firstly, we studied the influence of two ionic liquids, choline dihydrogen phosphate ([Ch][DHP]) and 1-butyl-3-methylimidazolium chloride ([C_4mim]Cl), on the SCOMT lysate for 12 hours by applying a storage temperature of 4 ºC or -80 ºC and whether the ionic liquids would increase the stability of the protein, evaluating its specific activity. A greater potential stabilizing effect was obtained using [C_4mim]Cl at 4 °C, with an activity recovery of about 350% over 12 hours. Then, crystallization tests of purified SCOMT fractions were carried out, using the vapor diffusion (Hanging Drop) and counter diffusion methods, where several factors were evaluated, namely, temperature (4 ºC and 20 ºC), concentration and composition of the precipitating agent solution (HEPES, pH=7.5, methyl-2,4-pentanediol and Caps, pH 10.5, Li_2SO_4, NaH_2PO_4/ K_2HPO_4) and the influence of S-adenosyl-L-methionine (SAM) and 3.5 -dinitrocatechol (DNC), a cofactor and a COMT inhibitor, respectively. By evaluating the various factors, we were able to conclude that better results were obtained at a temperature of 20 ºC, which corresponds to a precipitating agent solution composed of Caps, pH 10.5, Li_2SO_4, NaH_2PO_4/K_2HPO_4 and that the steam diffusion technique showed more promising results. In addition, a high concentration of precipitates was observed throughout the tests, mostly DNC and, in the minority, salts present in the solution of the precipitating agent. In a last step, the results obtained were classified, namely, distinguishing protein crystals from salt crystals, but due to their small size, X-ray identification was not possible. Thus, as an alternative, tests such as the absorption of dyes (Timol Blue and Coomassie Blue) were carried out and the Crush Test. These tests showed inconclusive results, since, due to the small size of the crystals, it was not possible to identify their nature with certainty.

Keywords

Crystallization; Inhibitors; Ionic Liquids; SCOMT; Stability.

Table of Contents

Chapter 1- Introduction 1

1.1 Catechol-*O*- methyltransferase 3

1.1.1 COMT Function 3

1.1.2 Isoforms: SCOMT and MBCOMT 4

1.1.3 Genetic Polymorphisms 5

1.1.4 SCOMT Stability 6

1.1.5 COMT Inhibitors 7

1.2 Biosynthesis and Recovery of Human Recombinant SCOMT 11

1.3 Protein crystallization 13

1.3.1 Thermodynamics of Protein Crystallization 13

1.3.1.1 Solubility 13

1.3.1.2 Phase diagram 15

1.3.2 Kinetics of Protein Crystallization 16

1.3.2.1 Nucleation 16

1.3.2.1.1 Homogeneous Primary Nucleation 17

1.3.2.1.2 Heterogeneous Primary Nucleation 20

1.3.2.1.3 Secondary Nucleation 21

1.3.2.2 Crystal growth 21

1.3.3 Conventional methods of protein crystallization 22

1.3.3.1 Sitting-drop vapor - diffusion 22

1.3.3.2 Hanging-drop vapor - diffusion 23

1.3.3.3 Microdyalisis 23

1.3.3.4 Counter-Diffusion 24

1.3.3.5 Liquid-liquid free-interface diffusion 25

1.3.4 COMT crystallization 25

Chapter 2 – Objectives 27

Chapter 3 - Materials and Methods 31

3.1 Materials 33

3.2 Recombinant SCOMT production and recuperation 34
3.3 Immobilized metal affinity chromatography 35
3.3 SCOMT enzymatic assay..... 35
3.4 Western-Blot..... 36
3.5 Crystallization studies 37
3.5.1 Hanging-drop vapor – diffusion 37
3.5.2 Counter-Diffusion 39
Chapter 4 - Results and Discussion.....41
4.1 SCOMT_6His purification assays 43
4.2 Studies for SCOMT stabilization 45
4.3 Screening of SCOMT crystallization conditions 48
4.3.1 Temperature and precipitating agent 48
4.3.2 Concentration of the precipitating agent solution..... 50
4.3.3 Influence of SAM and DNC.....51
4.3.4 Dye absorption test 53
Chapter 5 – Conclusions.....57
Chapter 6 – References.....61

List of Figures

Figure 1 - The *O*-methylation of a standard catechol by COMT.....3

Figure 2 - Physical map of the human COMT gene..... 4

Figure 3 - The tertiary structure of the COMT enzyme.....7

Figure 4- Representative structures of the “first generation” COMT inhibitors..... 8

Figure 5- Representative structures of the “second generation” COMT inhibitors.....10

Figure 6 - Representative structure of the Opicapone.....10

Figure 7 - Typical phase diagram for the crystallization of macromolecules..... 16

Figure 8 – Graph showing the total free energy as function of nucleus radius.....17

Figure 9 – Illustration showing tangential growth and normal growth.....22

Figure 10 – Illustration showing the sitting-drop-vapor diffusion method.....23

Figure 11 – Illustration showing the hanging-drop-vapor diffusion method.....23

Figure 12 – Illustration showing the microdialysis method.....24

Figure 13 – Illustration showing the counter-diffusion method..... 24

Figure 14 – Illustration showing the liquid-liquid free-interface diffusion method..... 25

Figure 15 – The SCOMT_6His chromatographic profile..... 44

Figure 16 –SDS-PAGE analysis (A) and Western Bolt (B) of the SCOMT..... 44

Figure 17 – SCOMT Lysate (Control) chromatogram at 4 °C.....45

Figure 18 – SCOMT Lysate (Control) chromatogram at -80 °C..... 45

Figure 19 – Chromatogram of SCOMT lysate at 4 °C where the sample consists of SCOMT lysate in IL-free stabilizing buffer.....46

Figure 20 – Chromatogram of SCOMT lysate at 4 °C where the sample consists of SCOMT lysate in (C_4min)(Cl) stabilizing buffer.....46

Figure 21 – Graphs that translates the specific activity at 4 °C and at -80 °C.....46

Figure 22 – Graphs that translates the specific activity recovery at 4°C and at -80 °C.....47

Figure 23 – Images captured from the Hanging Drop crystallization trials where the temperature of 20 °C was evaluated.....48

Figure 24 – Images captured from the Hanging Drop crystallization trials where the temperature of 4 ºC was evaluated.....49

Figure 25 – Images captured from the Counter Diffusion crystallization trials where the temperature was evaluated..... 49

Figure 26 – Hanging drop test, where 1:1 ratio was tested..... 50

Figure 27 – Hanging drop test, where 2:1 ratio was tested..... 50

Figure 28 – Images captured in the Counter Diffusion test, where the initial concentration of the precipitating solution was reduced by half.....51

Figure 29 – Images captured in the hanging drop test, where only SCOMT is present..... 52

Figure 30 – Image captured in the hanging drop test, where SCOMT+DNC.....52

Figure 31 – Image captured in the hanging drop test, where SCOMT+SAM.....52

Figure 32 – Image captured in the hanging drop test, where SCOMT+SAM+DNC..... 53

Figure 33 – Images captured in the hanging drop crystallization trials, where only SCOMT is present with dyes..... 54

Figure 34 – Images captured in the hanging drop test, where SCOMT+DNC is present with dyes..... 54

Figure 35 – Images captured in the hanging drop test, where SCOMT+SAM is present with dyes..... 55

Figure 36 – Images captured in the hanging drop test, where SCOMT+SAM+DNC is present with dyes.....55

Figure 37 – Microscopic images of crystals obtained.....56

List of Schemes

Scheme 1 – Scheme showing the types of nucleation..... 17

Scheme 2 – Scheme showing the two alternative pathways that lead from solution to solid crystal.....20

Scheme 3 – Diagram showing the main steps of SCOMT production and recovery..... 34

Scheme 4 – Diagram showing the main steps of SCOMT purification..... 35

Scheme 5– Diagram showing the main steps of Counter-Diffusion method..... 40

List of Equations

Equation 1 - Supersaturation formula.....13

Equation 2 - Chemical potential of a solute in a saturated solution.....14

Equation 3 - Chemical potential of a solute in a supersaturated solution.....14

Equation 4 - Association between the proportion of activities and concentration..... 14

Equation 5 - Simplified equation of equation 4..... 14

Equation 6 - Gibbs free energy formula..... 18

Equation 7 - Gibbs free energy formula derived from changes in surface area..... 18

Equation 8 - Gibbs free energy formula derived from changes in volume.....18

Equation 9 - Gibbs free energy considering that the embryo is spherical.....18

Equation 10 - Gibbs free energy given by derivatives..... 19

Equation 11 - Critical radius formula..... 19

Equation 12 - Nucleation rate adapted from the Arrhenius equation..... 19

Equation 13 - Simplified equation of equation 12.....19

Equation 14 – Association between the critical activation energy of the solution and the external surface.....20

Equation 15 – Interfacial tension.....20

Equation 16 - Secondary nucleation rate..... 21

List of Tables

Table 1- Affinity Constant and Maximum Enzymatic Rate of both COMT isoforms.....5

Table 2- The kinetic parameters of the COMT enzyme and its affinity to dopamine in the presence of inhibitors.....9

Table 3 - Solution compositions in the study of the influence of SAM and DNC and in the presence of dyes.....39

List of Abbreviations

(C_4mim)(Cl)	1-butyl-3-methylimidazolium chloride
(Ch)(DHP)	Choline dihydrogen phosphate
3-OMD	3-*O*-methyldopa
AADC	Aromatic Acid Decarboxylase
BIA 9-1067	Opicapone
BMG	Buffered Minimal Glycerol Medium
BMM	Buffered Minimal Methanol Medium
CADD	Computer Assisted Drug Discovery
CAPS	N-cyclohexyl-3-aminopropanesulfonic acid
CHES	N-Cyclohexyl-2-aminoethanesulfonic acid
CNS	Central Nervous System
CNT	Classical Nucleation Theory
COMT	catechol-*O*-methyltransferase
Cvs	Column volumes
DMSO	Dimethyl sulfoxide
DNA	Deoxyribonucleic Acid
DNase	Deoxyribonuclease
DNC	3,5-Dinitrocatechol
DTT	Dithiothreitol
E. coli	*Escherichia coli*
ED	Electrochemical Detection
EGTA	Ethylene glycol-bis(β-aminoethyl ether)-N,N,N′,N′-tetraacetic acid
EMA	European Medicines Agency
FDA	Food and Drug Administration
HEPES	4-(2-hydroxyethyl)-1-piperazineethanesulfonic acid

HPLC	High Performance Liquid Chromatography
ILs	Ionic Liquids
IMAC	Immobilized Metal Affinity Chromatography
K. pastoris	*Komagataella pastoris*
L-DOPA	Levodopa
MBCOMT	Membrane-bound form of catechol-*O*-methyltransferase
Mg^{2+}	Magnesium ion
NMR	Nuclear Magnetic Resonance
OD	Optical Density
OD600	Optical Density at 600 nm
PDB	Protein Data Bank
PEG	Polyethylene glycol
PSA	Ammonium persulfate
RNA	Ribonucleic acid
SAH	S-adenosyl- L-homocysteine
SAM	S-adenosyl-L-methionine
SAR	Structure Activity relationship
SCOMT	Soluble form of catechol-*O*-methyltransferase
SDS	Sodium dodecyl sulfate
SDS-PAGE	Sodium dodecyl sulfate–polyacrylamide gel electrophoresis
TEMED	Tetramethylethylenediamine
Tris	Tris(hydroxymethyl)aminomethane
Val108Met	Valine for a Methionine at codon 108
YPD	Yeast Extract Peptone Dextrose

Chapter 1- Introduction

1.1 Catechol-*O*- methyltransferase

The catechol-*O*-methyltransferase (COMT, E.C.2.1.1.6) is a monomeric enzyme that in the presence of magnesium cation (Mg^{2+}) catalyzes the transfer of a methyl group from the cofactor S-adenosyl-L-methionine (SAM) to the catechol substrate, thus resulting in *O*-methylated products and S-adenosyl- L-homocysteine (SAH) [1]. This enzyme was discovered in 1958 by Axelrod and Tomchick in rat liver extracts [2] and thereafter was found in bacteria, yeast, plants, insects, fish, amphibians, birds, and mammals [3].

In mammals, COMT is distributed throughout the body's organs and its highest activity levels have been found in the liver, kidneys, and intestinal wall [4]. This enzyme is also expressed in the prefrontal cortex and limbic system. Importantly, the liver is the most relevant site for the metabolism of circulating catechol-containing molecules [5]. In humans, besides its role in catecholamines catabolism, COMT has been implicated in the inactivation of catechol estrogen, catechol-containing xenobiotics, such as catechins and bioflavonoids, and indole intermediates from melanin metabolism [6]. COMT tissue distribution and substrate specificity support a putative protective role as an enzymatic barrier against exogenous catechol's by preventing their oxidation to *O*-quinones and the formation of electrophiles [6]. The catechol *O*-methylation seems to decrease the tendency for redox cycling and to increase lipophilicity facilitating the transmembrane transport out of the cell [6].

1.1.1 COMT Function

Recently, COMT has become the target of pharmacological studies [7–9], due to its possible involvement in some human diseases, such as Parkinson's disease, Alzheimer's disease, and schizophrenia. The major physiological function of COMT consists in the inactivation of biologically active or toxic catechol's, to promote the inactivation of neurotransmitters in the central nervous system and in the regulation of the dopaminergic and noradrenergic pathways.

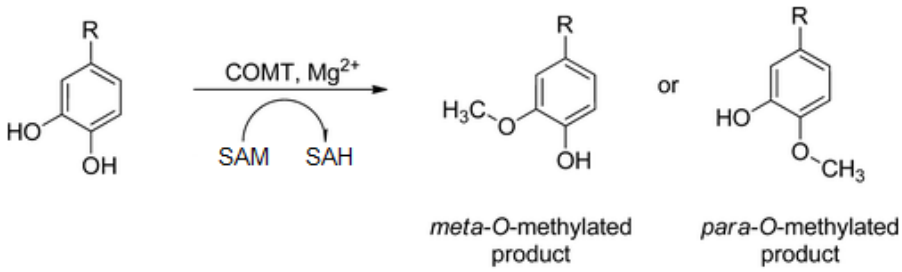

Figure 1 - The *O*-methylation of a standard catechol by COMT. SAM: S-adenosyl-L-methionine; SAH: S-adenosyl-L-homocysteine; Mg^{2+}: Magnesium (adapted from [4]).

As seen in Figure 1, mammalian COMT catalyzes the catechol substrate to form two isomers, *meta*- and *para*-*O*-methylated products. The proportion of *meta*- and *para*-*O*-methylated metabolite is very different between substrates, depending on the properties of the ring substituents [5]. In most cases, catechol substrates show clear preference for *meta*-*O*-methylation, especially for substrate with highly polar substituents [5]. However, for the substrate with an apolar substituent the amounts of *meta*- and *para*-*O*-methylates are in a 1:1 ratio. The presence of a nonpolar region in the catechol binding site of mammalian COMT may repel the binding of polar substrates in the orientation required for *para*-*O*-methylation, whereas nonpolar substrates may bind more randomly, resulting in the formation of nearly equal amounts of *meta*- and *para*-*O*-methylated products [5].

1.1.2 Isoforms: SCOMT and MBCOMT

A single gene has been found to encode two isoforms of the protein, a soluble form (SCOMT) and a membrane-bound form (MBCOMT) [10]. The gene is located on the q11.21 band of chromosome 22 and contains six exons [11]. Regarding codons, the first two are non-coding and consequently, the translation initiation codons for both isoforms are located only in the third codon [12]. Their expressions are regulated by two promoters, a shorter transcript of 1.3 kb translates to SCOMT, and a longer transcript of 1.5 kb translates to MBCOMT [5].

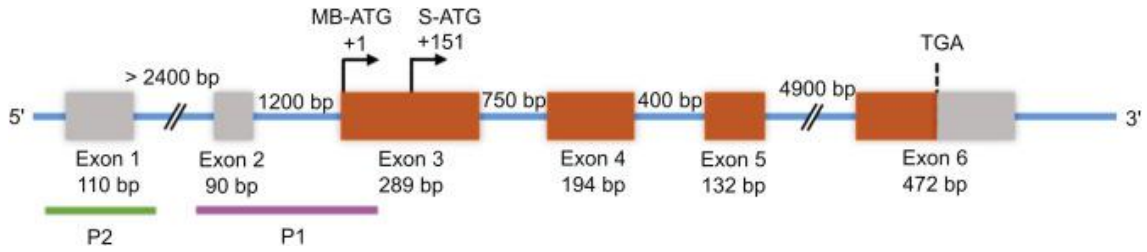

Figure 2 - Physical map of the human COMT gene (adapted from [5]).

The isoform MBCOMT, predominant in brain tissues, has a molecular weight of 30 kDa and a signal sequence located in the N-terminal region with 50 amino acids where it forms a membrane anchor associated with the rough endoplasmic reticulum membrane [13]. In contrast, SCOMT is distributed throughout all peripheral tissues and ubiquitous to several organs, with a molecular weight of 24.7 kDa, its composed by a total of 221 amino acids and it can be found in the cytoplasm [14].

Despite the kinetic similarities shared by both isoforms, the requirement for the co-factors Mg^{2+} and SAM and the substrate affinity is completely different [15]. MBCOMT is required to modulate the inactivation of dopaminergic and noradrenergic neurotransmitters such as dopamine, epinephrine, and norepinephrine [3]. On the other hand, SCOMT participates in the inactivation and detoxification of biologically active catechol molecule and their hydroxylated metabolites such as catechol estrogens, including 2-hydroxyestradiol, 2-hydroxyestrone, 4-hydroxyestradiol and 4-hydroxyestrone [16].

Table 1- Affinity Constant (K_M) and Maximum Enzymatic Rate (V_{max}) of both COMT isoforms for several catecholamines (adapted from [17,18]).

	MBCOMT		**SCOMT**	
	V_{max}	**K_M (µM)**	**V_{max}**	**K_M (µM)**
Dopamine	16.9 ± 0.5 min^{-1}	15.1 ± 0.9	37.2 ± 1.3 min^{-1}	207 ± 14
Norepinephrine	18.1 ± 0.2 min^{-1}	24.1 ± 0.7	34.9 ± 1.4 min^{-1}	369 ± 25
L- Dopa	12.2 ± 0.2 min^{-1}	266 ± 10	42.5 ± 1.5 min^{-1}	613 ± 35
DBA	22.2 ± 0.4 min^{-1}	30 ± 1.0	43.4 ± 2.2 min^{-1}	38.9 ± 4.1
Epinephrine	0.9 ±0.1 nmol/mg protein/h	4.8 ± 0.1	345 ± 78 nmol/mg protein/h	58 ± 4

The data shown in Table 1, clearly support the claims that MBCOMT is the isoform responsible for *O*-methylation at physiologically low concentrations of catecholamines, particularly in the central nervous system (CNS). On the other hand, SCOMT is primarily responsible for the *O*-methylation of catechol compounds in peripheral tissues at higher substrate concentrations [17].

1.1.3 Genetic Polymorphisms

More than 900 genetic variants for the COMT gene have been reported, but most of them showed no physiological importance. Human COMT has two polymorphic forms at amino acid 108 in SCOMT and amino acid 158 in MBCOMT, a low activity thermolabile form contains methionine (Met108/158) and a high activity thermostable form contains valine (Val108/158) [19]. The Met108/158 allele has been linked to increased risk of breast cancer [20], obsessive-compulsive disorder [21], schizophrenia [22] ,and increased sensitivity to pain [23], but it has also been associated to an improvement in prefrontal cognitive function, especially in

memory work [23]. This polymorphism is caused by the change from guanine to adenine in the genetic code and is associated, for example, with Parkinson's disease [24].

In humans, COMT activity is distributed in 3 levels, low (COMT ^{LL}), intermediate (COMT ^{LH}) and high (COMT ^{HH}) [25]. The Met108/158 variant is associated with low enzyme activity, is more prone to active site distortion and protein aggregation, and there is a decrease in thermal stability, while the Val108/158 variant is associated with high activity [26]. However, there are other polymorphisms in the COMT gene, such as the polymorphism reported by Lee and his collaborators (Ala72Ser in MBCOMT and Ala22Ser in SCOMT) where was reported the association between a functional polymorphism and the activity of the COMT enzyme [27]. The Ala/Ser variation in the COMT gene was associated with a greater reduction in enzyme activity than the well-studied Val/Met polymorphism [27].

1.1.4 SCOMT Stability

In recent decades, the use of “therapeutic” proteins has allowed the treatment of various diseases, but aggregation and misfolding continue to be a recurring problem as they play an important role in cell dysfunction and tissue damage, which in turn lead to several physiological effects [28]. The tendency of aggregation induces a decrease in biological activity and reduces the efficiency of separation techniques, since protein aggregation causes artifacts in most biophysical techniques [29]. To overcome this difficulty, several purification techniques have been developed to improve protein stability in solution and, therefore, recuperation yields and purification degrees [30]. To avoid loss of enzymatic activity, it is necessary to control several parameters such as pH and ionic strength. Specifically, ionic strength affects an enzyme's activity by altering the enzyme's stability and solubilities [30]. The effects of salts on stability become more relevant with more hydrophilic enzymes, so our research group in a previous work established that SCOMT can be stable in a buffer that contains NaCl, with a concentration of 150 mM [31]. Furthermore, the pH is essential for the maintenance of SCOMT activity and therefore, its ideal value is stablished between 7.5 and 8 [32]. Also, as this protein is highly unstable and rapidly loses its activity during isolation and storage [33], temperature is one of the main critical parameters that affects COMT activity. This low stability could be related with the oxidation of -SH-free cysteine groups and consequently the formation of disulfide bonds intra or intermolecular [34]. In addition, the presence of cofactors is mandatory for the function of an enzyme and, therefore, the cofactors SAM and Mg^{2+} are essential for the catalytic activity of SCOMT, as they reduce cysteine oxidation and therefore prevent protein inactivation. [34]. Lastly, stabilizers have been used to protect proteins against loss of activity and thermal denaturation such as

sugars, divalent metals, glycerol, and amino acids [35]. Sugars have the function of stabilizing the native protein structure through the protective action of the protein hydration shell [36], divalent metals contribute to the catalytic process through their ability to attract or donate electrons [37], glycerol is known to displace the set from native proteins to more compact states and inhibits protein aggregation during refolding [38], amino acids are known as natural osmolytes that can stabilize proteins [39] and finally ionic liquids due to the various combinations of ions that allow different physicochemical properties show a unique ability to preserve the stability and conformation of proteins and prevent their aggregation [40]. Specifically, for SCOMT, it was described by our research group that this protein is stable in a solution containing cysteine, trehalose, and glycerol [41]. It has also been shown that low temperatures, specifically 4ºC, favor correct protein folding and less aggregation, leading to an increase in the results of SCOMT activity [41].

1.1.5 COMT Inhibitors

For the design of new molecules, namely the synthesis of new inhibitors for the COMT, it is important to know the three-dimensional structure of the protein. Thus, COMT is composed of a single domain of an α/β structure, consisting of a core of seven strands of β-sheets, of which β1-β6 are parallel and β7 is antiparallel, sandwiched between two helix sheets α as verified in Figure 3 [42]. The active site of COMT is equivalent to the binding domain of S-adenosyl-L-methionine and some amino acids such as Lysine and Proline, which have a special relevance for the binding of substrate, water, and Mg^{2+} [25]. Amino acid residues such as Lysine 144 accept a proton from the hydroxyl group and residues such as Proline 174 form hydrophobic walls that determine the selectivity of COMT for the substrate [43].

Figure 3 - The tertiary structure of the COMT enzyme (PDB: 6I3C) as an example (adapted from [44]).

Regarding the inhibitors that have been studied over the years, these have been grouped into three generations. The first COMT inhibitors were described in the 1970s by Guldberg Marsden [24] which has led to a breakthrough in the treatment of Parkinson's disease [45]. These "first generation" of inhibitors are primarily formed by catechol and pyrogallol chemical skeletons [46]. These molecules contain a catechol ring in their structure or some bioisoteric moiety, including flavonoids, benzoic acids, catechol ketones and pyrogallol derivatives [47]. This class of COMT competitive substrates also includes 2-hydroxyoestrone, quercetin, rutin, gallic acid, caffeic acid, U-0521, and non-catecholic compounds such as ascorbic acid, tropolones, 8-hydroxyquinoline derivatives, 3-hydroxylated pyrones, and pyridines [48]. *In vitro* studies showed that these compounds have little selectivity and potency for COMT [49]. Also, inhibitors such as tropolone and pyrogallol present low efficacy *in vivo* and are toxic [50].

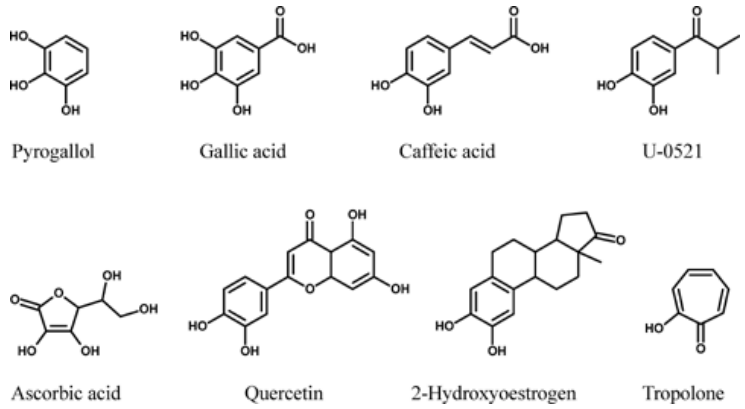

Figure 4- Representative structures of the "first generation" COMT inhibitors (adapted from [49]).

To overcome the difficulties presented by the first-generation inhibitors, a second generation of inhibitors was developed. Considering information taken from several structure–activity relationship (SAR) studies, the best results were obtained when a nitro group is present at position 5 of the catechol ring, leading to high potency and selectivity, and consequently better pharmacokinetics performance than several other tested substituents [51]. One of the most promising nitro-catechol inhibitors of COMT was 3,5-dinitrocatechol (3,5-DNC) which despite showing good results *in vitro*, during *in vivo* studies this compound showed high toxicity and low pharmacokinetic rate, which prevented its clinical use [52].

Therefore, several highly potent, selective, and orally active inhibitors have been studied to assess safety *in vitro*, *in vivo*, and even clinical trials [53]. Nitrocatechol molecules are generally described kinetically as COMT inhibitors [17]. Since they are poor substrates for the enzyme, they compete with the substrate for the binding site and are not competitive with the SAM binding site [54]. These molecules show greater selectivity for COMT than for other enzymes involved in catecholamine metabolism [55]. According to the data obtained from *in*

vitro and *in vivo* studies, only Tolcapone, Nitecapone and Entacapone were fully characterized in additional studies [4]. They were the most promising compounds of this class, inhibiting SCOMT with a K_i of 1.02, 0.30, 0.27 nM for, and the MBCOMT K_i values of 2.00, 1.37, and 0.29 nM for Nitecapone, Entacapone, and Tolcapone, respectively [17]. These values may differ slightly to the different experimental conditions, enzyme source preparations, and assay conditions. In humans, despite the compounds structural similarities they inhibited COMT in different manners. Nitecapone, mostly affected COMT duodenum activity, while Entacapone showed higher inhibition in the liver and erythrocytes [56], being both considered strictly peripheral inhibitors. In contrast, Tolcapone exhibited higher potency and a longer period of action than the Entacapone, it is considered a central COMT inhibitor, due to its ability to cross the blood-brain barrier and influence brain COMT activity [57]. However, Tolcapone is associated with increases in the plasmatic levels of liver transaminases, causing severe hepatoxicity [58]. Currently, only Tolcapone and Entacapone are approved for clinical use [42].

Table 2- The kinetic parameters (K_M, V_{max}) of the COMT enzyme and its affinity to dopamine in the presence of inhibitors (K_i, K_{cat})(adapted from [17]).

Substrate	COMT	Source	V_{max} (min^{-1})	K_M (μM)	Inhibitor (10 - 30 nM)	K_i (nM)	K_{cat} (min^{-1})
Dopamine (300 uM)	S	Recombinant	37.2 ± 1.3	207 ± 4	Entacapone	0.30	31.1
	MB		16.9 ± 0.5	15.1 ± 0.9		2.00	14.1
	S		37.2 ± 1.3	207 ± 4	Nitecapone	1.02	26.2
	MB		16.9 ± 0.5	15.1 ± 0.9		1.37	17.8
	S		37.2 ± 1.3	207 ± 4	Tolcapone	0.27	30.9
	MB		16.9 ± 0.5	151 ± 0.9		0.29	17.4

The use of these inhibitors with Carbidopa, a commercial aromatic L-amino acid decarboxylase (AADC) inhibitor, significantly improved the bioavailability of L-DOPA, as there is a reduction in the levels of 3-*O*-Methyldopa (3-OMD) and thus, an increase in the levels of L-DOPA reaching the brain [31].

In recent years, new inhibitors have been designed using computational tools based on atomic interactions of protein inhibitors by computer-assisted drug discovery (CADD) approaches [59]. So, new nitrocatechol inhibitors were found, namely nebicapone and BIA-3-335 [60]. In 2016, Palma and coworkers were able, for the first time, to complex the structure of the soluble form of COMT with a new inhibitor, called BIA 8-176, based on docking simulations and molecular orbital calculations [61].

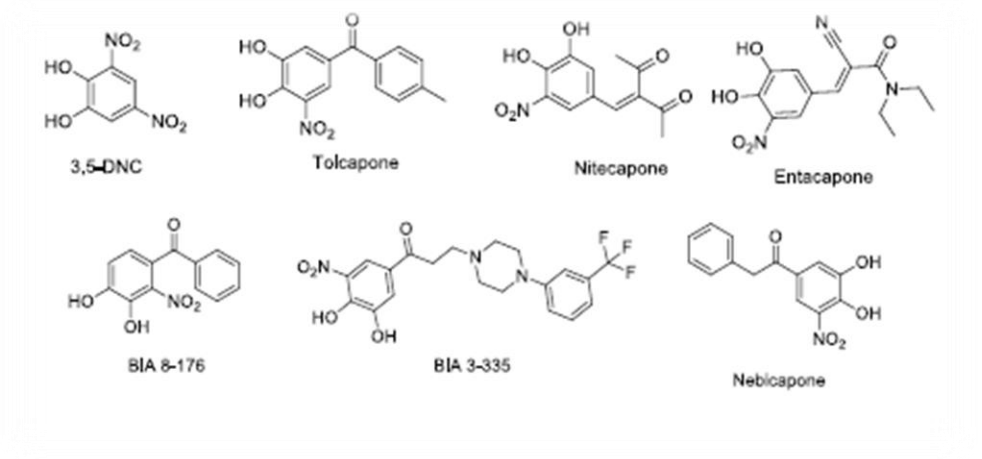

Figure 5- Representative structures of the "second generation" COMT inhibitors (adapted from [62]).

Recently, the Portuguese Pharmaceutical Company Bial – Portela & C[a], SA has developed a new inhibitor, Opicapone (BIA 9-1067) [63]. This molecule was approved in 2016 by the European Medicines Agency (EMA) and in 2020 by the Food and Drug Administration (FDA) as an adjuvant to L-DOPA therapy in the treatment of Parkinson's disease [64,65]. This third generation of COMT inhibitors showed a longer duration of action, a higher binding affinity and bioavailability *in vivo* and allowed for once-daily administration, with stable plasma L-DOPA levels being observed [58,66]. While Opicapone mainly inhibited erythrocyte COMT activity, but cannot penetrate the blood-brain barrier, so it is considered a strictly peripheral inhibitor [67].

Since the inhibitors discovered to date only alleviate the symptoms of Parkinson's disease and other neurological diseases, there is a constant need for improvement and therefore new classes of COMT inhibitors continue to be explored [68].

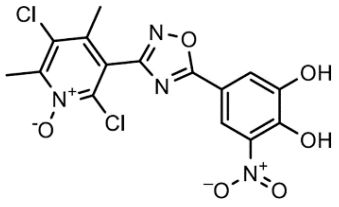

Opicapone

Figure 6 - Representative structure of the Opicapone (adapted from [69]).

1.2 Biosynthesis and Recovery of Human Recombinant SCOMT

Since the pharmacological relevance of COMT was discovered, the focus of the biotechnological community became the development and optimization of bioprocesses capable of obtaining large amounts of COMT with a high degree of purity for further structural and functional studies. The first successful case of isolation of COMT from a rat liver was done by Axelrod and collaborators, employing a combination of ammonium sulphate fractioning with gel filtration [2]. Over the years, several productions and recovery methodologies have been described and, due to technological advances in recombinant DNA technologies, there has been an optimization that allowed higher production yields and an easier recovery of human recombinant proteins [70]. The ability of the host to process and translate the transcribed RNA and simultaneously modify the translated protein with the correct folding and bioactivity makes the choice of the expression system a very relevant factor. For the biosynthesis of the soluble form of COMT (SCOMT), different expression systems have been used, such as transfected mammalian cells [43], insect cells (via mammalian vectors and baculovirus) [43], plant cells (via potyvirus) [71], prokaryotic cells such as *Escherichia coli* (*E. coli*) [45] and yeasts, such as *Komagataella pastoris* (*K. pastoris*) [72]. Of these expression systems used, it is important to highlight *E. coli* and *K. pastoris*. As for *E. coli*, more specifically the BL21 strain, it is widely used for the expression of recombinant proteins due to the lack of two specific proteases (*Ion* and *ompT*), it prevents the degradation of heterologous proteins [73]. One BL21 derived strain in particular, *E. coli* BL21 (DE3), has been used to successfully express several homologous and heterologous soluble proteins, including COMT [73]. In relation to yeasts systems, these are desirable eukaryotic hosts to produce heterologous proteins as they have rapid growth rates, high cell densities and provide a well-developed variety of genetic tools [74]. In recent years, the yeast *K. pastoris* has been used as an expression system to produce recombinant proteins because, being a unicellular microorganism, it is easily manipulated and cultivated and, as a eukaryote, it is capable of post-translational modifications such as proteolytic processing, folding, disulfide bond formation and glycolization [72]. Typically, *K. pastoris* has two alcohol oxidase genes, AOX 1 and AOX 2 where the former is much more transcribed than the latter, which makes it advantageous when induction is affected by methanol [75].

Regarding the main isolation steps, several chromatographic approaches have been made during the last decades for the purification of COMT from crude cell lysates. The first purification strategy for this enzyme was developed by Lundtröm and collaborators based on ion exchange chromatography onto Q- Sepharose matrices. [76]. More recently, several strategies have been described in the literature, such as the combination of affinity

chromatography and anion exchange chromatography [77] or the association of immobilized metal affinity chromatography (IMAC) plus gel filtration [78]. Interesting results were obtained using a butyl-Sepharose resin followed by gel filtration, allowing the recovery of SCOMT in a highly purified state, but the application of ammonium sulfate was shown to have a negative effect on the biological activity of SCOMT, thus compromising its stability and the development of further structural studies [79]. Regarding the recovery of bioactivity and the degree of purity, a value of 23% and 3.90 fold was obtained, respectively [79].

Immobilized metal affinity chromatography (IMAC) has been widely used as a method to isolate proteins from fermentation broths or other biological sources [80]. Several proteins have already been purified using IMAC, such as human growth hormone [80], immunoglobulins [81] or membrane proteins such dehydrogenase/reductase SDR family member 7 (DHRS7, SDR34C1, retSDR4) [82]. IMAC is a separation technique where metal ions (such as Cu^{2+}, Ni^{2+}, Zn^{2+}, Co^{2+} and Fe^{3+}), are trapped in a solid chromatographic support that serve as affinity ligands for various proteins tagged with a histidine tag [83,84]. In general, the biomolecules are retained in IMAC using an equilibrium buffer without imidazole or at low concentrations between 1 to 10 mM and the elution is usually achieved by increasing the imidazole concentration [75]. Usually, the buffers contain a specific concentration of NaCl to reduce nonspecific electrostatic interactions. In IMAC, through the competition with nickel ions, the imidazole is responsible for eluting the proteins and when present at low concentrations in the binding buffer, it may prevent the binding of host proteins with exposed histidines, allowing the removal of contaminants in the flowthrough during the injection of the sample [75]. This methodology is extremely efficient and selective for the direct capture of hexahistidine tagged SCOMT from recombinant *K. pastoris* lysates [75]. Regarding the bioactivity recovery and the degree of purity, these output presents a value of 57.4% and 81 fold, respectively, showing the best results reported for the capture of this protein [75].

1.3 Protein crystallization

Crystallization is a very efficient method for purifying macromolecules, although it is mostly used in x-ray crystallography to determine the three-dimensional structure of proteins [85]. Protein crystallization consists of two major steps: nucleation and crystal growth [86]. Nucleation is defined as a process of aggregation of protein molecules, being highly dependent on the supersaturation of the protein solution as well as on the thermodynamic conditions of the system, including temperature, pH, and solution composition [86]. The effect that each of these parameters has on the behavior of the protein phase can be represented in a phase diagram, where the most favorable operating conditions for crystal growth can be identified [86].

For crystallization to occur, the protein must be inherently crystallizable, i.e., when the periodic intermolecular contacts necessary for self-assembly into a regular network cannot be formed under any circumstances, any protein-rich phases that separate from the protein solution will not form crystals. In addition, thermodynamic conditions must establish the necessary conditions for crystallization, that is, in a system of a given chemical composition, there must be a stable, protein-rich phase in the form of a crystal, in equilibrium with its growth solution [87].

1.3.1 Thermodynamics of Protein Crystallization

1.3.1.1 Solubility

The solubility of a solution can be described as the maximum amount of a given solute that can be dissolved in a certain solvent. For crystallization of a given protein to occur, supersaturation must be achieved, that is, the concentration of the protein in solution must be above its solubility, or in other words, it must be above the equilibrium concentration, under given conditions of temperature, pH, and solution composition [88].

Supersaturation is normally characterized by the difference between the chemical potentials of the solute in a supersaturated solution and in a saturated solution designated by μ and $\mu_{S,}$ respectively [88]:

$$\mu - \mu_s = RT \ln \frac{a}{a_s}$$

Equation (1)

Where R represents the perfect gas constant, T represents the temperature, a and a_s represent the activity in the supersaturated solution and in the saturated solution,

respectively. The chemical potential of a solute in a saturated and supersaturated solutions is given by the following equations, respectively:

$$\mu = \mu_i^0 + RT \ln a$$

Equation (2)

$$\mu_s = \mu_i^0 + RT \ln a_s$$

Equation (3)

Where μ_i^o represents the standard chemical potential of species *i*.

The ratio of activities can be associated with concentration as verified in the following equation:

$$\frac{a}{a_s} = \frac{a}{a^*} = \frac{\gamma C}{\gamma^* C^*}$$

Equation (4)

The γ and C terms represent, respectively, the activity coefficient and the protein concentration in the solution. Terms with an asterisk refer to equilibrium. As a rule, the ratio of activity coefficients in saturated and supersaturated solutions is considered to have a value of 1 because it is assumed that they are dilute solutions, that is, ideal solutions. The simplified equation (5) is demonstrated by:

$$S = \frac{C}{C^*}$$

Equation (5)

The solubility of a solution can be affected by several parameters such as the concentration of the precipitating agent, temperature, and pH. In the case of SCOMT, in addition to these factors, since the protein is in a solution with various compounds such as cysteine, trehalose and glycerol, it is important to note that their presence will also affect the solubility of the protein. About precipitating agents, these can be divided into three categories: salts, polymers, and organic solvents [88].

Salts are the most chosen precipitating agents because of their low cost. In turn, protein molecules and salt ions need solvent molecules around them to be dissolved, that is, protein molecules and ions compete for solvent molecules. Regarding how salts affect the solubility of a protein, we can highlight two processes, *salting -in* and *salting - out*. In the *salting -in* process, there is a low concentration of ions in solution, i.e., their addition will contain the several ionic charges of the target biomolecule and weaken the forces of attraction between protein molecules and, therefore, inhibit aggregation and formation of protein crystals. In

the *salting - out* process, there is a high concentration of ions and thus, they compete with the protein molecules for the solvent molecules, leading to the aggregation of the protein molecules and thus, formation of crystals [86].

Polymers produce volume exclusion effects that also induce the separation of macromolecules from the solution. Because polymeric precipitants do not have a consistent conformation like proteins, they writhe and twist randomly in solution and take up much more space than they should. This leads to less solvent space available for the macromolecules, which then segregate, aggregate, and finally form a solid state, usually crystals [89].

Organic solvents reduce the dielectric constant of the medium, which in effect allows two proteins to come close together. As the concentration of the organic solvent increases, the attraction between the macromolecules increases and, in turn, the solvent becomes less effective, and the solid state is favored [90]. Organic solvents are used at low temperatures (at or below 0 °C) and must be added very slowly like alcohols, acetone, or other water miscible organic solvents. Since they are volatile substances, care must be taken when preparing crystallization solutions to avoid loss of solution. The ionic strength must be kept low and any means available must be sought to protect against denaturation [91].

Temperature is also an important parameter as it influences the variation of the acid/base reaction constant of the protein side chains and has a significant effect on the ionic strength which is greater the lower the ionic strength present in the solution. Because proteins are very sensitive, they must be handled between 0 °C and 40 °C, as they denature outside this range. Proteins are normally crystallized at room temperature or 4 °C [86].

The pH by changing the ionic attraction force between amino acids influences the interaction between protein molecules, therefore, it is an input to be considered in the crystallization of proteins. Typically, crystallization occurs in a short pH range, and it is necessary to maintain the value so that the protein structure remains folded. At the isoelectric point (charge is zero) protein precipitation occurs rather than crystallization because at this point protein solubility is minimal [86].

1.3.1.2 Phase diagram

The phase diagram is an interesting tool for protein crystallization because it gives information on the physical state of the protein (liquid, crystalline or amorphous solid) as a function of the systems relevant parameters, such as temperature, pH, ionic strength, protein concentration, precipitating agent and other additives [92].

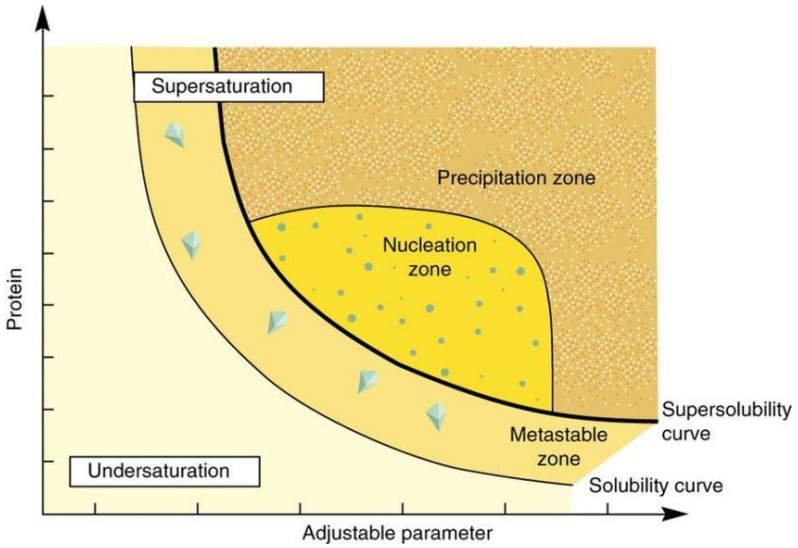

Figure 7 - Typical phase diagram for the crystallization of macromolecules (adapted [93]).

Undersaturated zone depicted below the solubility curve shows conditions where the protein is soluble and therefore will not crystallize. Above the solubility curve, there is the metastable zone where crystal growth is promoted, but there will be no spontaneous formation of new nuclei. The nucleation zone is defined by spontaneous nucleation, where supersaturation is moderate. Finally, we have the precipitation zone where supersaturation is very high, thus the protein precipitation occurs, forming amorphous aggregates [92].

Due to the number of tests and the time required to develop a phase diagram, it is not very common to find it in the literature, so protein crystals are mostly obtained through a trial-error approach, where precipitant solutions, additives and buffer solutions are mixed with the protein solution to promote crystal formation, resulting in low reproducibility [92].

1.3.2 Kinetics of Protein Crystallization

1.3.2.1 Nucleation

The first step of the protein crystallization process is nucleation. This step is crucial because many of the characteristics of the crystals (e.g., size, number…) are established during this phase. As nucleation is stochastic, that is, its state is indeterminate and originates from random events, and everything happens at a molecular scale, it becomes very difficult to study it, both experimentally and theoretically [86].

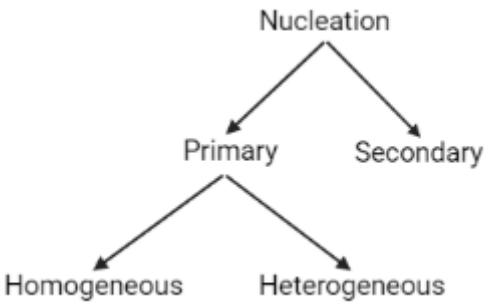

Scheme 1 – Scheme showing the types of nucleation (adapted [94]).

Nucleation is divided into two categories, primary nucleation and secondary nucleation, the primary being subdivided into two other categories, homogeneous nucleation, and heterogeneous nucleation [95]. Primary nucleation takes place without any crystalline matter, in contrast, secondary nucleation takes place in a supersaturated medium and in the presence of crystalline matter from the protein under study [94]. The homogeneous process is the result of the random movement of molecules and, as a rule, results in their orderly arrangement. This process occurs more in materials of high purity and high supersaturations environments [86]. Heterogeneous nucleation is favored by the presence of external agents, particularly the crystallizer wall or impurities present in the solution [94].

1.3.2.1.1 Homogeneous Primary Nucleation

In the classical theory of nucleation (CNT), there is a first phase where molecules begin to associate and form aggregates that later evolve into embryos. Then there is a reorganization of the embryos and an increase in their size, until they reach a critical size and form nuclei [96]. Afterwards, the molecules that are free in the solution are absorbed at the surface, thus increasing their size by incorporation into the crystal lattice. The occurrence of nucleation is only possible when very high levels of supersaturation are achieved, that allowing's to overcome the barrier of activation energy [97].

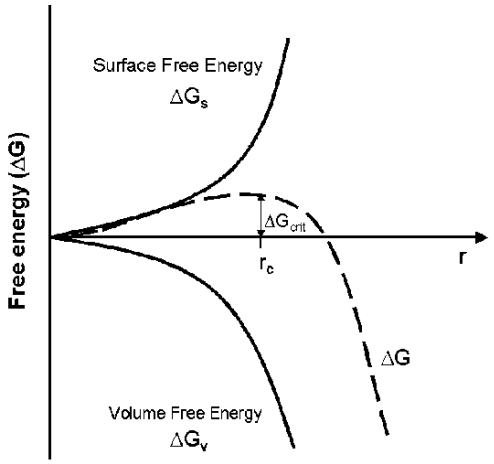

Figure 8 – Graph showing the total free energy, ΔG, as function of nucleus' radius (adapted [98]).

Gibbs free energy, at constant temperature and pressure, is expressed by [99]:

$$\Delta G = V\Delta G_V + A\Delta G_A$$

Equation (6)

Where V is the volume and A is the surface area of the nucleus. ΔG_V and ΔG_A represent the change in Gibbs free energy derived from changes in volume and surface area, respectively. ΔG_A can be simplified as the surface tension, σ, which lies between the developing crystalline surface and the supersaturated solution, as follows [99]:

$$\Delta G_A = \sigma$$

Equation (7)

ΔG_V is related to the molecular affinity of solutes and depends on the solute concentration in the solution, as verified in the following equation [99]:

$$\Delta G_V = -\left(\frac{kT}{V_M}\right)\ln\left(\frac{a}{a^*}\right)$$

Equation (8)

The k represents the Boltzmann constant, T the temperature, V_M the volume of a solute molecule, and the a and a^* are the solute activities in solution and in equilibrium, respectively.

Assuming that the activity coefficient of a solute is 1 and that the embryo in question is spherical, we can assume that the change in Gibbs free energy is given by [99]:

$$\Delta G = -\frac{4}{4\pi r^3}\left(\frac{kT}{V_M}\right)\ln\left(\frac{C}{C_S}\right) + 4\pi r^2\sigma$$

Equation (9)

Where r represents the embryo radius and C and C_S represent the solute concentration in solution and the equilibrium solute concentration, respectively.

Since the embryo's radius, surface tension, temperature, solute molecular volume, and Boltzmann 's constant are expressed by physically positive values, Equation 9 suggests that the Gibbs free energy increases with the embryo's radius [99]. According to the literature, if the solute concentration is lower than the equilibrium concentration then crystallization will not be spontaneous and external work must be provided for the embryo to grow [85,99]. Conversely, when the ratio of solute concentrations in solution and in equilibrium is greater than 1, the variation in the volume of the embryo leads to a reduction in the Gibbs free

energy, that is, a maximization of the variation in the free energy relative to embryo size [85,99].

Gibbs free energy can be given by the derivative, with respect to the radius of the embryo, given by the following equation:

$$\Delta G = \frac{16\pi\sigma^3}{3\left[\left(\frac{kT}{V_M}\right)\ln\left(\frac{C}{C_S}\right)\right]^2}$$

Equation (10)

On what:

$$r^* = \frac{2\sigma}{\left(\frac{kT}{V_M}\right)}\ln\left(\frac{C}{C_S}\right)$$

Equation (11)

The r^* is the critical radius and corresponds to the radius of the embryo when the Gibbs free energy is maximum. The maximum Gibbs energy is also called the critical activation energy.

Using an Arrhenius equation we can express the nucleation rate, *J*, that is, the number of nuclei formed per unit volume and time:

$$J = A\ exp\left(-\frac{\Delta G^*}{kT}\right)$$

Equation (12)

The A is a pre-exponential factor, which is replaced by $\frac{2D}{d^5}$, where *D* represents the diffusion coefficient and *d* represents the diameter of the solute molecule [99].

Assuming that the nucleus is a sphere, the nucleation rate is given by:

$$J = A\ exp\left(-\frac{16\pi\sigma^3}{3\left\{\left[\left(\frac{kT}{V_M}\right)\ln\left(\frac{C}{C_S}\right)\right]^2 kT\right\}}\right)$$

Equation (13)

The CNT is based on the fluctuation and origin of the nucleation barrier to explain the nucleation mechanism, but disagreements between experimental values of nucleation rates and theoretical predictions have been evidenced [85]. To explain these differences, the two-step nucleation mechanism emerged. This mechanism shows that at first the solute, in supersaturated solution, forms agglomerates or a dense liquid phase, and later, it reorganizes itself to develop an ordered structure [100].

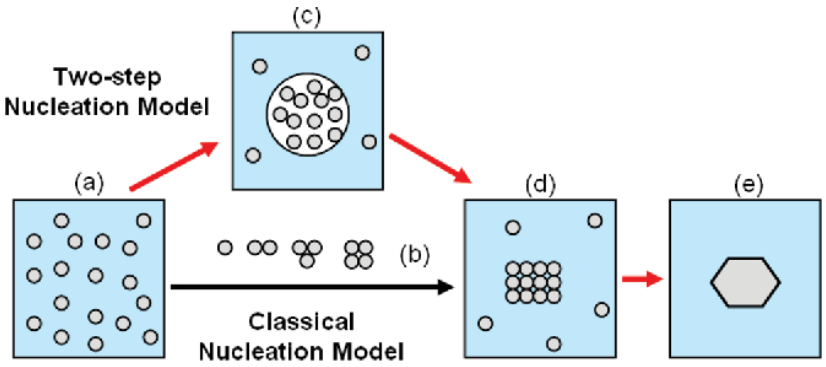

Scheme 2 – Scheme showing the two alternative pathways that lead from solution to solid crystal: (a) supersaturated solution; (b) ordered subcritical clustering of solute molecules, proposed by the classical nucleation theory; (c) liquid agglomerate of solute molecules, dense precursor proposed by the two-step nucleation theory; (d) ordered crystalline nuclei; (e) solid crystal (adapted [98]).

1.3.2.1.2 Heterogeneous Primary Nucleation

During heterogeneous primary nucleation, crystals form on surfaces such as dust particles, crystallizer wall, air-solution interface or deliberately added mold particles while homogeneous primary nucleation occurs in the absence of heterogeneous particles in a clear solution [101].

This nucleation normally needs lower supersaturation and activation energy [102]:

$$\Delta G^{*\prime} = \emptyset \Delta G^{*}$$

Equation (14)

The $\emptyset$ represents the interfacial tension dependent factor between an external surface and the solution, which normally has a value lower than 1. This value is determined by the contact angle, and can be derived as [102]:

$$\emptyset = \frac{(2 + \cos\theta)(1 - \cos\theta)^2}{4}$$

Equation (15)

The contact angle between solid and liquid is represented by θ. When θ is equal to 180º, $\Delta G^{*\prime}$ has the same value as ΔG^{*}, that is, the critical activation energy is not reduced by the external surface. On the other hand, when θ is less than 180° the outer surface reduces the energy at the beginning of nucleation and at the critical activation energy [102].

1.3.2.1.3 Secondary Nucleation

Secondary nucleation only occurs in the presence of crystals of the protein under study, i.e., it can run with a supersaturation much lower than the supersaturation necessary to cause primary nucleation [97].

The secondary nucleation rate can be determined using the following equation [103]:

$$J = kn'(C - C_S)^i(MF)^j$$

Equation (16)

$k_n{}'$ represents the secondary nucleation rate constant, *MF* the determining factor for secondary nucleation, without considering supersaturation, and i and j are the potency indices [97]. The *MF* factor can refer to the agitation speed, friction, or breakage, that is, it depends on the parameter that controls the secondary nucleation [103].

1.3.2.2 Crystal growth

In a supersaturated solution, after the formation of a stable nucleus (size greater than the critical size), growth follows, in which the crystal can reach dimensions perceptible to the naked eye. Protein crystals grow by mechanisms like those existing in crystals of inorganic materials, although the rates are very different. The growth of protein crystals in solution occurs by sequential addition of layers [104]. Regarding the addition of layers to the surface, it is carried out through two processes called: tangential and normal growth to the face. Normal surface growth arises from the formation of new layers or growth units that have edges on the step where new molecules can adhere tangentially [104]. Tangential growth contributes to the lateral extension of the surface layers [104].

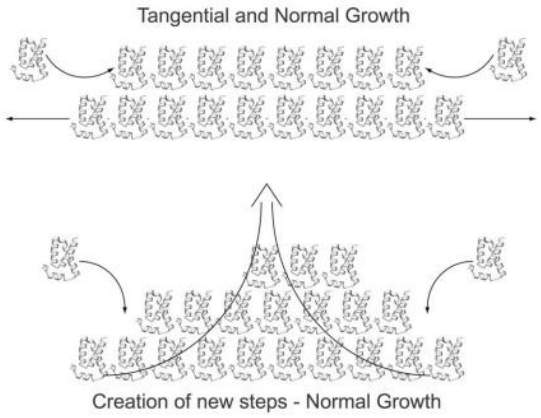

Figure 9 – Illustration showing the tangential growth by adding molecules to the edges of the steps and the normal growth where there is the creation of nascent layers on top of those already present (adapted[104]).

1.3.3 Conventional methods of protein crystallization

The growth of protein crystals must be carried out in some physical mechanism that allows the researcher to change the solubility of the protein and the properties of the mother liquor, using strategies to promote supersaturation such as, for example, changing the temperature or pH, addition or salt removal or evaporation. Currently, these mechanisms use micro techniques almost exclusively, so crystallization assays with a given array of conditions can be performed with volumes of just a few microliters or less [86].

1.3.3.1 Sitting-drop – vapor diffusion

In this technique, a drop composed of a protein solution is mixed with a precipitant solution and placed in vapor equilibrium with a reservoir composed of the precipitant solution with a higher concentration. Typically, the droplet contains a lower reagent concentration than the reservoir. To reach equilibrium, water vapor leaves the droplet and ends up in the reservoir. As water leaves the droplet, the sample experiences an increase in relative supersaturation. Both the sample and the reagent increase in concentration as the water leaves the droplet into the reservoir. Equilibrium is reached when the concentration of reagent in the droplet is approximately the same as in the reservoir [105].

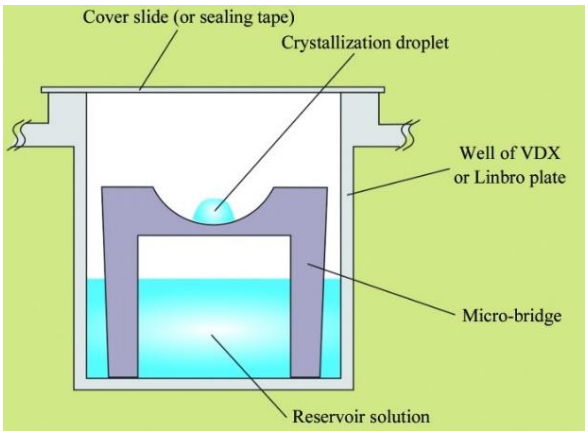

Figure 10 – Illustration showing the sitting-drop vapor-diffusion method (adapted [86]).

1.3.3.2 Hanging-drop – vapor diffusion

The droplet and reservoir components, and the physical equilibrium process, are the same here as for the sitting- drop method. The exception is that the protein droplet is suspended in a siliconized glass coverslip over the shell rather than resting on a surface [106].

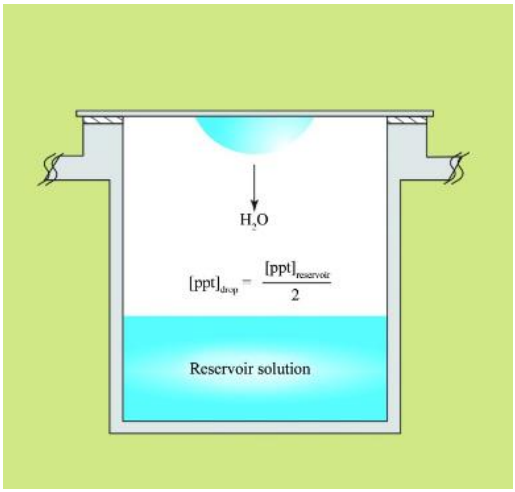

Figure 11 – Illustration showing the hanging-drop vapor-diffusion method (adapted [86]).

1.3.3.3 Microdyalisis

In the microdialysis crystallization method, the sample is separated from the precipitant solution by a semipermeable membrane. The semipermeable membrane allows the passage of small molecules, such as salts, additives, and other crystallization reagents, but prevents biological macromolecules from crossing the membrane. Sample crystallization occurs due to diffusion of the crystallization reagent out of or into the sample at constant sample concentration [107].

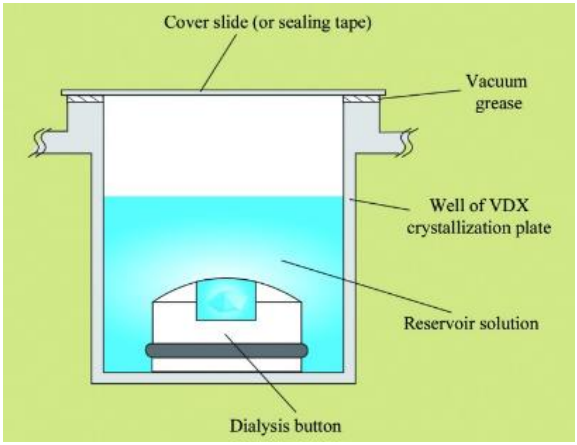

Figure 12 – Illustration showing the microdialysis method (adapted [86]).

1.3.3.4 Counter-Diffusion

In this technique, a capillary containing the protein solution is pressed against a gel and sealed at its distal end and then impregnated with a precipitant solution. Over time, the precipitant diffuses through the capillary to establish a gradient. In this way, the protein is exposed to a concentration gradient of precipitant. Due to the interaction of diffusion and precipitant crystallization, the dynamics of the process in the capillary is much more complex, but this only increases the probability of nucleation and more orderly growth. When the technique is successful, it is possible to observe microcrystals where the precipitant concentration is highest, i.e., near the surface of the gel, and large crystals near the distal end of the capillary [86].

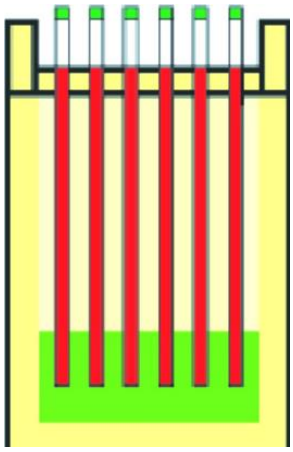

Figure 13 – Illustration showing the counter-diffusion method (adapted [86]). The protein solution is shown in red, and the gel saturated with the precipitant solution is shown in green.

1.3.3.5 Liquid-liquid free-interface diffusion

The counter-diffusion method was based on this ancient method which consists of a protein solution placed over a precipitant solution in a tube or capillary with a reduced diameter. Diffusion across the interface, mostly of the precipitant, induces nucleation and crystal growth [86].

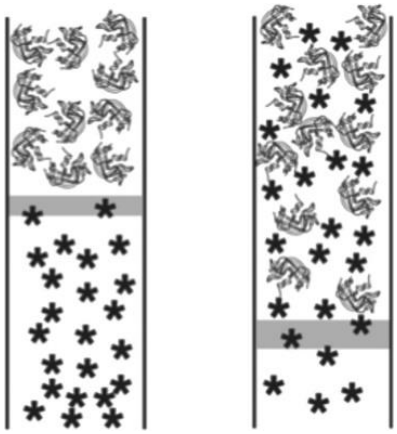

Figure 14 – Illustration showing the liquid-liquid free-interface diffusion method (adapted [86]).

1.3.4 COMT crystallization

One of the first requirements for crystallization assays is that we must start from a pure, stable, and homogeneous protein solution. In this way, as reported by our research group, SCOMT maintains its stability in a buffer constituted by $MgCl_2$, cysteine, trehalose, and glycerol [40]. Typically, cysteine plays a role in the formation of intramolecular and intermolecular disulfide bonds that are essential for maintaining the native three-dimensional structure [40]. Trehalose is often reported in the literature as a protein denaturation protector [40], glycerol as a thermostabilizer [40] and $MgCl_2$ is added because it contains the cofactor (Mg^{2+}) required for the enzymatic activity [40].

Once the protein solution is defined, the next step is the precipitation solution. Precipitating solutions are generally composed of a precipitating agent (salts, organic solvents, or polymers) and a buffer. According to the literature, most of the precipitating solutions in relation to the crystallization of SCOMT have salts or polymers as the precipitating agent. About salts, Na_2HPO_4 [108], NaCl [109], Li_2SO_4 [110] and $(NH_4)_2SO_4$ [109] are widely used. The presence of $MgCl_2$ is also found in several studies, but it does not act as a precipitating agent, but as a cofactor of the enzyme. Regarding polymers, the most used is polyethylene glycol (PEG), a hydrophilic polymer of ethylene oxide. Within this polymer, the most used are PEG 1000 [109], PEG 1500 [108], and PEG 3350 [108].

As for buffers, the most used are Tris-HCl [110], CHES [109], CAPS [110] and NaH_2PO_4/K_2HPO_4 [110] as they provide pH stability the enzyme is more stable (pH between 7.5 and 8). In some cases, SAM is added to protect the protein against thermal inactivation and denaturation [78]. Regarding the optimal pH of the protein, it is described between 7.5 and 8 to mimic the physiological environment [32]. Regarding storage temperature, as described by our group, the optimal temperature is 4 ºC as it favors the correct protein folding [41].

Once the requirements for the crystallization tests have been defined, an attempt is made to obtain the SCOMT crystal. Several crystal structures of this enzyme have already been demonstrated in the literature using different inhibitors, for example, Ellermann and his colleagues studied ribose-modified bisubstrate inhibitors COMT crystal structures from mouse tissues that that confirmed the predicted binding mode but displayed subtle alterations at the ribose-binding site. [111]. Czarnota and colleagues determined X-ray crystal structures and NMR backbone assignments of human SCOMT ternary complexes containing dinitrocatechol, SAM, or sinefungin [44]. Harrison and his colleagues studied the inhibitors 3-hydroxy-4-pyridinones and 5-hydroxy-4-pyrimidones in crystal structures of COMT with the cofactors SAM and Mg^{2+} which showed satisfactory results to understand its inhibition mechanisms [112].

Chapter 2 – Objectives

Given that COMT rapidly loses its biological activity during the recovery and storage process, it is considered a highly unstable and thermolabile enzyme and is therefore stabilized through specific molecules capable of increasing its thermodynamic stability, thus preventing its denaturation and loss of activity. In recent years, ionic liquids (ILs) have demonstrated a unique ability to preserve the stability and conformation of proteins and prevent their aggregation, due to the different combinations of ions that give them different physicochemical properties. Once the optimal conditions of activity, stability and purity of the protein are guaranteed, carrying out crystallization tests is the next step, where information on its three-dimensional structure is obtained.

Therefore, the objective of this work was to study the effect of the interaction of ionic liquids on the enzymatic activity of SCOMT and to screen the crystallization conditions from purified SCOMT fractions. This major objective is divided into three parts:

1. Production, recovery, and purification of rS-COMT protein from *Komagataella pastoris* cells.
2. Improve the stability of rS-COMT, where different temperatures, precipitating agents and ionic liquids are studied.
3. Investigate rS-COMT crystallization conditions using conventional protein crystallization methods.

Graphical Abstract:

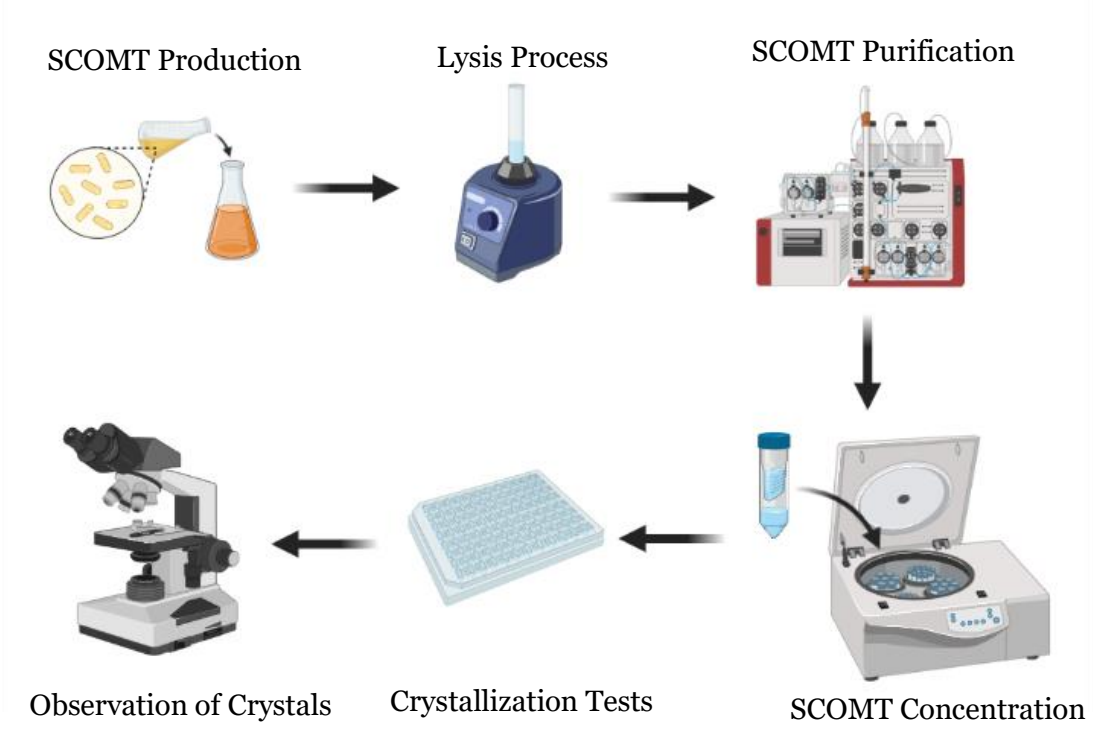

Chapter 3 - Materials and Methods

3.1 Materials

Ultrapure reagent-grade water was obtained with a Mili-Q system (Millipore/Waters). Yeast nitrogen base, glucose, agar, yeast extract, peptone, biotin, di-potassium hydrogen phosphate, potassium dihydrogen phosphate monobasic, phosphoric acid, dimethyl sulfoxide (DMSO), methanol, sulphuric acid, sodium hydroxide, sodium dodecyl sulfate (SDS), ammonium persulfate (PSA), tetramethylethylenediamine (TEMED), magnesium di-chloride ($MgCl_2$), ethylene glycol-bis(β-aminoethyl ether)-N,N,N′,N′-tetraacetic acid (EGTA), dithiothreitol (DTT), S-adenosyl-L-methionine (SAM), epinephrine (bitartrate salt), deoxyribonuclease (DNase), protease inhibitor cocktail, L-cysteine, zeocin, choline dihydrogen phosphate ([Ch][DHP]), sucrose, sodium chloride, imidazole, trehalose, 1-butyl-3-methylimidazolium chloride ($[C_4mim]Cl$), monosodium phosphate, paraffin, dipotassium phosphate, lithium sulfate, glycerol, D,L-metanephrine hydrochloride, agarose, citric acid monohydrate and glass beads (500 μm) were purchased from Sigma Chemical Co. (St. Louis, MO, USA). Acrylamide 40%/Bis solution was obtained from Bio-Rad (Hercules, CA). Tris(hydroxymethyl)aminomethane (Tris) and CAPS was obtained from Fisher Scientific (Epson, United Kingdom). The NZYcolour Protein Marker II was purchased from NZYTech (Lisbon, Portugal). Anti-rabbit IgG alkaline phosphatase secondary antibody was purchased from GE Healthcare Biosciences (Uppsala, Sweden), while the monoclonal rabbit COMT antibody was acquired from Abcam (Cambridge, England). All chemicals used were of analytical grade, commercially available, and applied without further purification.

3.2 Recombinant SCOMT production and recuperation

The construction of the expression vector pPICZα-hSCOMT, the *K. pastoris* transformation and selection for positive clones was previously done by our research group [31]. Unless otherwise noted, recombinant SCOMT was produced generally as shown in Scheme 3 and in more detail according to the following protocol. Cells containing the expression construct were grown at 30 °C in YPD plates and then a single colony was inoculated in 100 mL of BMG medium in 500 mL shake flasks. Subsequently, cells were grown at 30 °C and 250 rpm overnight when the cell density at 600 nm (OD_{600}) typically reached 6.0. Afterwards, since the inoculation volume was fixed to achieve an initial OD_{600} of 1.0, an aliquot of the fermentation in the medium BMG was collected and centrifuged at room temperature for 5 min. After centrifuging the cells and ensuring all glycerol was removed, the cells were resuspended in the induction medium (BMM) and added to 500 mL shake-flasks to a total volume of 100 mL. The fermentations were carried out for 24 h at 30 °C and 250 rpm and were supplemented with methanol at a final concentration of 5% (v/v). Then, the cells were harvested by centrifugation (1500 × g, 10 min, 4 °C) and stored at −20 °C until use. The cell suspensions were lysed in equilibrium buffer (150 mmol L^{-1} NaCl, 10 mmol L^{-1} DTT, 50 mmol L^{-1} Tris, 1 mmol L^{-1} $MgCl_2$, pH 8.0) at a ratio of 1:2:2 (1 g cells, 2 mL lysis buffer and 2 g glass beads). *K. pastoris* lysis was accomplished through the application of a sequential procedure involving glass beads consisting of 7 cycles of vortexing (1 min) with 1 min of interval on ice. After the lysis process was completed, the mixture was centrifuged (500 g, 5 min, 4 °C) and DNase I was added (250 μgmL^{-1}). After the solid-liquid extraction, the supernatant was removed, and the pellet obtained was resuspended in the chromatographic binding buffer (500 mmol L^{-1} NaCl, 50 mmol L^{-1} Tris, 1 mmol L^{-1} $MgCl_2$ and 5 mmol L^{-1} imidazole at pH 7.8).

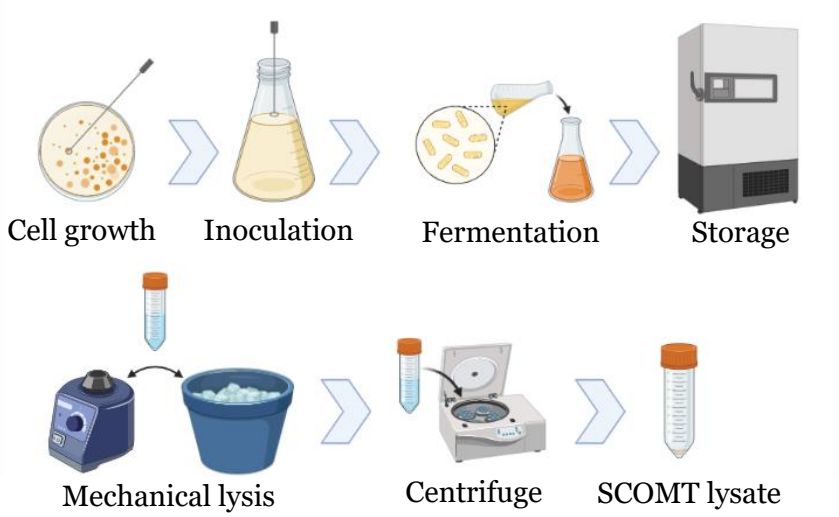

Scheme 3– Diagram showing the main steps of SCOMT production and recovery.

3.3 Immobilized metal affinity chromatography

The IMAC operation conditions were optimized previously by our research group [75]. Unless otherwise stated, the column HisTrap™ FF crude (5 mL) was initially equilibrated with 500 mmol L^{-1} NaCl, 50 mmol L^{-1} Tris, 1 mmol L^{-1} $MgCl_2$ and 5 mmol L^{-1} imidazole to pH 7.8. Aliquots of resuspended pellet in equilibration buffer (diluted 1:2), were applied onto the column using an injection volume of 500 µL at a flow rate of 0.5 mL min^{-1}. After elution of the unretained species, imidazole concentration was increased to 50 mmol L^{-1} at 1 mL min^{-1} in a stepwise mode under 5 column volumes (CVs). Subsequently, the stepwise mode was applied at 70 mmol L^{-1} of imidazole concentration, followed by a step to 300 mmol L^{-1} of imidazole. Finally, the imidazole concentration in the elution buffer was increased to 500 mmol L^{-1}.

In all chromatographic runs, the conductivity, pH, pressure, temperature as well as absorbance at 280 nm, to follow the protein concentration, were continuously monitored. Fractions were pooled according to the chromatograms obtained, collected in tubes containing a stabilizing solution (150 mmol L^{-1} NaCl, 50 mmol L^{-1} of Tris, 15 mmol L^{-1} of cysteine, 1 mmol L^{-1} $MgCl_2$, 5 mmol L^{-1} trehalose, 5% of glycerol and 10 mmol L^{-1}, 1-butyl-3-methylimidazolium chloride ([C_4mim]Cl)), concentrated and desalted with Vivaspin concentrators (10.000 MWCO) and conserved at 4 ºC until further analysis, as shown in Scheme 4.

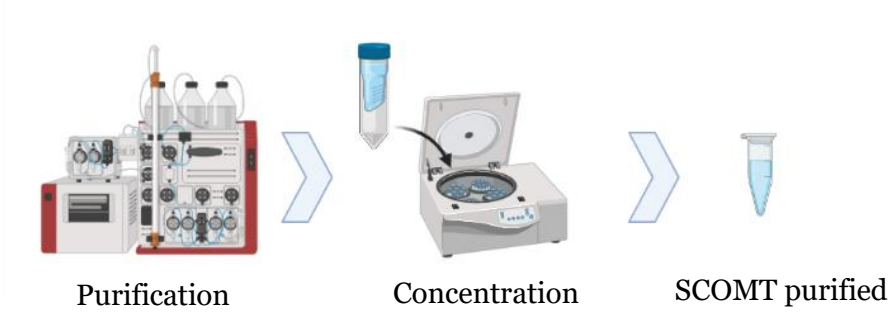

Scheme 4– Diagram showing the main steps of SCOMT purification.

3.3 SCOMT enzymatic assay

The experiments of activity were designed to evaluate the methylating efficiency of recombinant SCOMT by measuring the amount of metanephrine formed from epinephrine in the different fractions obtained from the IMAC runs [113]. For the SCOMT enzymatic assay, an aliquot of 150 µgmL^{-1} of the SCOMT resuspended pellets and purified extracts was incubated in 5 mmol L^{-1} sodium phosphate buffer (pH 7.8) containing 0.2 µmol L^{-1} $MgCl_2$, 2 mmol L^{-1} EGTA, 250 µmol L^{-1} SAM and 1 mmol L^{-1} epinephrine in a total sample volume

of 1 mL. Reactions were carried out at 37 ºC for 15 min and were stopped by incubation in ice following the addition of 2 mol L^{-1} 200 µL perchloric acid. The samples were centrifuged at 6000 rpm for 10 min, the supernatants were filtered and were subsequently injected into a HPLC system with a coulometric detector [113].

Briefly, the chromatographic analysis was performed using a HPLC Agilent 1260 system (Agilent, Santa Clara, USA) equipped with an autosampler, and quaternary pump coupled to an ESA Coulchem III detector (Milford, MA, USA). Chromatographic separation was achieved on an analytical column Zorbax 300SB C18 RP analytical column (250 × 4.6 mm i.d. 5 µm) (Agilent, Santa Clara, California, USA). The chromatographic method was developed using as mobile phase containing 0.1 mol L^{-1} NaH_2PO_4, 0.024 mol L^{-1} citric acid monohydrate, 0.5 mmol L^{-1} sodium octyl sulfate and 9% (v/v) acetonitrile. The column effluent was monitored by a coulometric detector, which was equipped with a 5011 high sensitivity dual electrode analytical cell (electrodes I and II) using a procedure of oxidation/reduction (analytical cell #1: +410 mV; analytical cell #2: –350 mV). The method sensitivity was set at 1 µA, the flowrate applied was 1 mL min^{-1} and the column temperature was setting at 30 ºC. The chromatograms were obtained by monitoring the reduction signal of the working electrode where metanephrine retention time was around 8.8 min. Finally, the metanephrine content in samples was measured using metanephrine standards (1–15 nmol mL^{-1}) as a calibration control [113].

3.4 Western-Blot

Total protein was resolved by 12% SDS-PAGE gel at 95 V for 1h30 at room temperature in the Running Buffer (Glycine 190 mM, Trizma-base 25 mM, SDS 1 mL, Mili-Q H_2O), and then, electro-transferred to a Polyvinylidene Difluoride membrane (GE Healthcare, Sweden) at 0.75 A for 1h45 in the transference buffer (CAPS 10x, Methanol, Mili-Q H_2O). Membranes were blocked for 1 h in a 5% (w/v) milk solution and incubated overnight with a rabbit polyclonal antibody against SCOMT (GE Healthcare Biosciences), diluted at 1:1000, at 4 ºC with constant stirring. The membranes were then washed in TBS-T buffer [Tris (0.2M), NaCl (1.4 M) and H_2O, pH 7.6] and incubated with a polyclonal antibody anti-rabbit (GE Healthcare Biosciences), diluted 1:10000, for 1 h at room temperature with constant stirring. Finally, the membranes were washed with TBS-T buffer, exposed to ECL substrate for 5 minutes protected from light and visualized on the Molecular Imager FX (Bio-Rad, Hercules, USA) [114].

3.5 Crystallization studies

SCOMT crystallization has been carried out by several research groups, which mostly use methods such as Hanging Drop and Micro-batch and temperatures of 4 ºC and 20 ºC. In the different studies, what differs most is the different types of precipitating agents used [44,115]. Due to the protein concentrations obtained in the experiments (depending on various factors in production and purification, the concentration values were not fixed but were between 0.5 and 4.5 mg/ml), the protocol suggested by Rutherford and his collaborators was adopted [78]. To the SCOMT solution composed of about 3 mg protein/ml, 50 mM Tris–HCl, pH 7.5, 150 mM NaCl, 1 mM $MgCl_2$, 15 mM cysteine, 5 mM trehalose, 5% glycerol and 10 mM [C_4mim]Cl, 50 mM SAM and 50 mM DNC was incubated for 1 h at room temperature prior to all crystallization trials. As mentioned in point 1.1.4, SAM and $MgCl_2$ are essential for catalytic activity as they reduce cysteine oxidation and therefore prevent protein inactivation. In addiction: sugars, amino acids and glycerol are used to protect the protein against loss of activity and thermal denaturation. The crystallization tests were carried out with the precipitating solution consisting of 0.1 M Caps, pH 10.5, 0.2 M Li_2SO_4 and 1.2 M NaH_2PO_4/0.8 M K_2HPO_4 at room temperature (~20 ºC) and for a temperature of 4 °C the precipitating solution was constituted by 0.1 M HEPES, pH=7.5 and 35% methyl-2,4-pentanediol. At the end, the assays are stored in a temperature-controlled incubator (20 °C) or in a cold room (4 °C).

3.5.1 Hanging-drop vapor – diffusion

This procedure was done on a VDX Plate [106]. The VDX Plate is a 24 well plate manufactured from clear polystyrene. The VDX Plate is typically sealed with High Vacuum Grease and Siliconized 22 mm Circle or Square Glass Cover Slides. Rows of the plate are labeled A-D and columns are labeled 1-6 on the VDX Plate. First, the buffer (0.1 M Caps or 0.1M HEPES) is prepared with milli-Q water. Then, the solution of the precipitating agent (0.2 M Li_2SO_4 and 1.2 M NaH_2PO_4/0.8 M K_2HPO_4 or 35% methyl-2,4-pentanediol) is prepared in the buffer and filtered using a 0.22 μm syringe filter. Then, Dow Corning® Vacuum Grease is placed around the wells. A volume of 600 μL of the reservoir solution (0.1 M Caps, pH 10.5, 0.2 M Li_2SO_4 and 1.2 M NaH_2PO_4/0.8 M K_2HPO_4 or 0.1 M HEPES, pH=7.5 and 35% methyl-2,4-pentanediol), i.e., the precipitating agent solution, is pipetted into the wells and 2 μL of the protein solution and 2 μL of the precipitating solution are placed on siliconized circles cover slides with a diameter of 22 mm and later, with the help of the micropipette, the solution is mixed. Finally, the plate is coated with aluminum foil to protect SAM from light and is placed in a temperature-controlled incubator (20 ºC) or in a cold room (4 °C) for later observation of the results in a stereomicroscope model SMZ1500, equipped with a Nikon DS-Fi3 digital camera where images were taken using the *NIS-Elements Advanced*

Research program. Results were first observed 2 days after the test and from the first observation they were examined every 5 days.

Several conditions were studied:

- Temperature and precipitating agent

  20 ºC - The precipitating solution consisted of 0.1 M CAPS, 1.2 M NaH_2PO_4/0.8 M K_2HPO_4, pH= 10.5 and 0.2 M Li_2SO_4. As the tests were performed using equal volumes of the protein (2 μL) and reservoir solution (2 μL) in the drop, the final concentration of the reservoir solution is 0.05 M CAPS, 0.6 M NaH_2PO_4/0.4 M K_2HPO_4, pH= 10.5 and 0.1 M Li_2SO_4 and the final protein concentration is 1.5 mg/ml (since this value varies depending on the production and purification processes, the initial concentration value of 3 mg/ml is used as a reference).

  4 ºC - The precipitating solution consisted of 0.1 M HEPES, pH=7.5 and 35% methyl-2,4-pentanediol. As the tests were performed using equal volumes of the protein (2 μL) and reservoir solution (2 μL) in the drop, the final concentration of the reservoir solution is 0.05 M HEPES, pH=7.5 and 17,5% methyl-2,4-pentanediol and the final protein concentration is 1.5 mg/ml.

- Concentration of the precipitating agent solution

  Proportion 1:1- Tests were carried out using equal volumes of the protein (2 μL) and reservoir solution (2 μL) in the drop, where the final concentration of the reservoir solution is 0.05 M CAPS, 0.6 M NaH_2PO_4/0.4 M K_2HPO_4, pH= 10.5 and 0.1 M Li_2SO_4 and the final protein concentration is 1 .5 mg/ml (since this value varies depending on the production and purification processes, the initial concentration value of 3 mg/ml is used as a reference).

  Proportion 2:1- Tests were carried out varying the proportion of the protein (4 μL) and the reservoir solution (2 μL) in the drop, where the final concentration of the reservoir solution is 0.03 M CAPS, 0.4 M NaH_2PO_4/0.27 M K_2HPO_4, pH= 10.5 and 0.07 M Li_2SO_4 and the final protein concentration is 2 mg/ml.

- Influence of SAM and DNC and the presence of Thymol Blue and Coomassie Blue dyes to differentiate between protein crystals and salt crystals (About 3 mg protein/ml, 50 mM Tris–HCl, pH 7.5, 150 mM NaCl, 1 mM $MgCl_2$, 15 mM cysteine, 5 mM trehalose, 5% glycerol, 10 mM [C_4mim]Cl) and only the presence of SAM and DNC varies (see Table 3).

Table 3- Solution compositions in the study of the influence of SAM and DNC and in the presence of dyes.

	No Dyes	Thymol Blue	Coomassie Blue
SCOMT	About 3 mg protein/ml, 50 mM Tris–HCl, pH 7.5, 150 mM NaCl, 1 mM $MgCl_2$, 15 mM cysteine, 5 mM trehalose, 5% glycerol, 10 mM $[C_4mim]Cl$	About 3 mg protein/ml, 50 mM Tris–HCl, pH 7.5, 150 mM NaCl, 1 mM $MgCl_2$, 15 mM cysteine, 5 mM trehalose, 5% glycerol, 10 mM $[C_4mim]Cl$ and 1 ul of Thymol Blue solution	About 3 mg protein/ml, 50 mM Tris–HCl, pH 7.5, 150 mM NaCl, 1 mM $MgCl_2$, 15 mM cysteine, 5 mM trehalose, 5% glycerol, 10 mM $[C_4mim]Cl$ and 1 ul of Coomassie Blue solution
SCOMT + DNC	Protein solution more 50 mM DNC	Protein solution more 50 mM DNC and 1 ul of Thymol Blue solution	Protein solution more 50 mM DNC and 1 ul of Coomassie Blue solution
SCOMT + SAM	Protein solution more 50 mM SAM	Protein solution more 50 mM SAM and 1 ul of Thymol Blue solution	Protein solution more 50 mM SAM and 1 ul of Coomassie Blue solution
SCOMT + SAM + DNC	Protein solution more 50 mM SAM and 50 mM DNC	Protein solution more 50 mM SAM and 50 mM DNC and 1 ul of Thymol Blue solution	Protein solution more 50 mM SAM and 50 mM DNC and 1 ul of Coomassie Blue solution

3.5.2 Counter-Diffusion

This procedure was done on a MASTERBLOCK® 96 Deep Well [116] and is generally illustrated in Scheme 5. To begin with, the 0.5% w/v agarose gel was prepared with 0.1 M CAPS pH=10.5 and placed on the hot plate until the agarose dissolved. Then, 200 µl of the protein solution was added and the BLAUBRAND® 2 µl capillaries were placed in the well to fill the capillaries with the protein solution by capillary action. Then, 600 µl of the agarose gel solution was placed in each well and allowed to cool. After this step, the capillaries were placed with the protein solution on the already hardened agarose gel and 600 µl of the precipitating agent solution was also pipetted into the wells. Then, the top of the capillary was covered with Sealing wax plates, and the well was filled with paraffin so as not to let the precipitating agent solution evaporate. Finally, the plate is coated with aluminum foil to protect SAM from light and is placed in a temperature-controlled incubator (20 ºC) for later observation of the results in a stereomicroscope model SMZ1500, equipped with a Nikon DS-Fi3 digital camera where images were taken using the *NIS-Elements Advanced Research* program. Results were first observed 2 days after the test and from the first observation they were examined every 5 days.

The following conditions were studied:

- Temperature and precipitation agent

  20 ºC - The precipitating solution consisted of 0.1 M CAPS, 1.2 M NaH_2PO_4/0.8 M K_2HPO_4, pH= 10.5 and 0.2 M Li_2SO_4.

  4 ºC - The precipitating solution consisted of 0.1 M HEPES, pH=7.5 and 35% methyl-2,4-pentanediol.

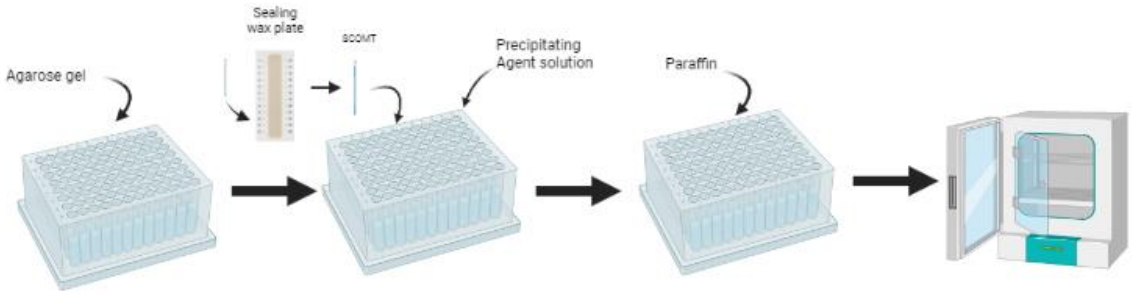

Scheme 5– Diagram showing the main steps of Counter-Diffusion method.

Chapter 4 - Results and Discussion

4.1 SCOMT_6His purification assays

Given the need to obtain high yields of SCOMT for crystallization tests, it is necessary to employ a biotechnological laboratory platform to produce SCOMT with an acceptable degree of purity [31]. *K. pastoris* can produce proteins with therapeutic properties in concentrations ranging from milligrams to grams per liter [75]. As a methylotrophic yeast, *K. pastoris* has a stronger and more regulated alcohol oxidase (AOX) promoter where high levels of transcription are induced by methanol [75]. Considering previous studies developed by our research group, SCOMT biosynthesis was successfully performed in a *K. pastoris* expression system, using the plasmid pPICZα-hSCOMT as construct [75]. Thus, the first part of this work consisted in the production and subsequent validation of the SCOMT lysis efficiency. For production, we use the conditions and methodologies described in section 3.2. The resulting pellets were lysed using the previously mentioned protocol (section 3.2) with a total protein concentration between 7 and 10 mg/ml [75]. To confirm that the lysis was efficient, an SDS-PAGE and Western blot analysis was performed both on the obtained supernatant (S) and on the corresponding pellet (I) (Figure 16). Using a specific antibody against SCOMT, an immunoreactive band was found at approximately 25 kDa [14]. Considering that the molecular weight of SCOMT is approximately 25 kDa, our results suggest that the detected band corresponds to the target enzyme.

IMAC has emerged over the past decade as one of the most widely methods used on a laboratory scale for the isolation of proteins from fermentation broths, culture supernatants and other biological sources, demonstrating high selectivity [80]. In general, biomolecules are retained in IMAC using binding buffer without imidazole or at low concentrations and elution is generally achieved by increasing the concentration of imidazole [117]. In IMAC, by competing with nickel ions, imidazole is responsible for eluting proteins, and it is preferable to use it at low concentrations in the binding buffer as it can prevent the binding of host proteins with exposed histidine's, allowing the removal of contaminants in the flow during sample injection [117]. According to work done by our research group SCOMT purification strategy is done using a stepwise gradient elution in a crude HisTrapTM FF (5 mL) according to the protocol mentioned in section 3.3 [75].

Firstly, the binding and elution conditions described previously [75] were applied to purify our protein. The chromatogram obtained is shown in Figure 15, in which the peak marked with the arrow is where the protein mostly elutes and the composition of the buffer in this step is 500 mmol L^{-1} NaCl, 50 mmol L^{-1} Tris, 1 mmol L^{-1} $MgCl_2$ and 300 mmol L^{-1} imidazole to pH 7.8.

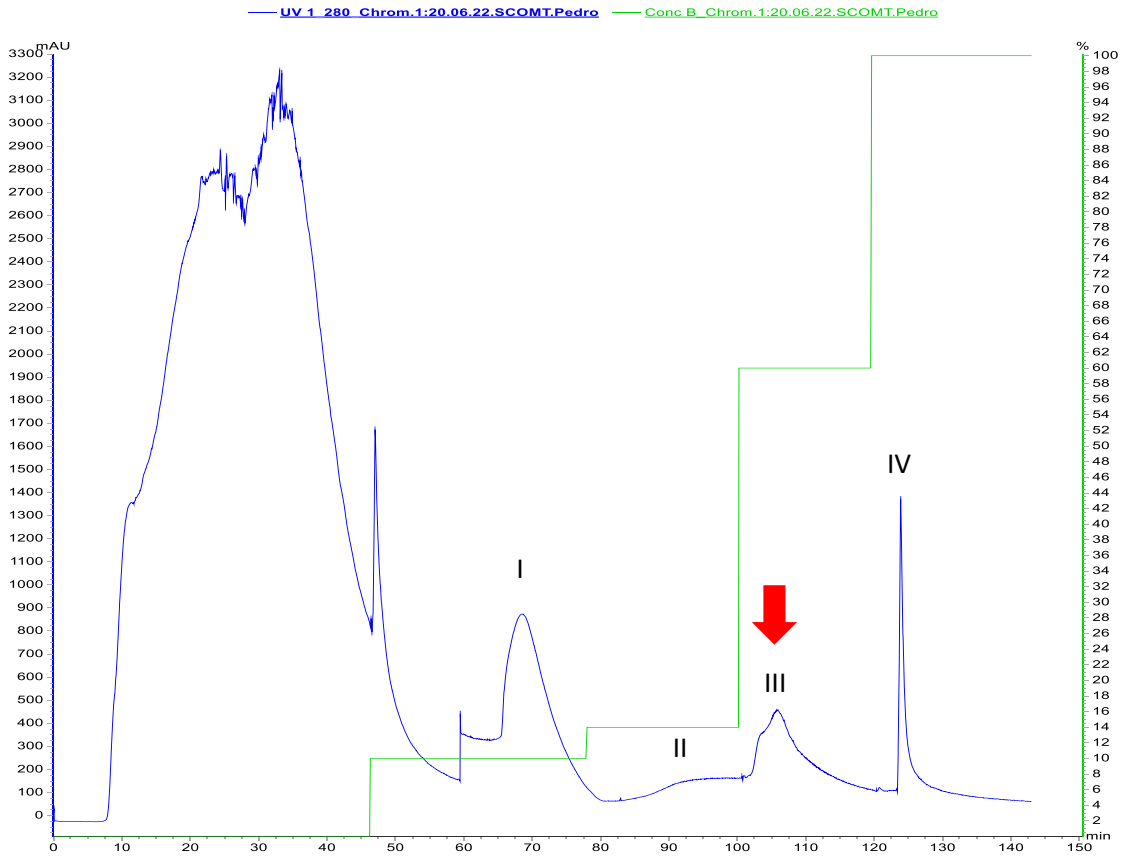

Figure 15 – The SCOMT_6His chromatographic profile using an imidazole gradient elution mode. Imidazole elution was carried out initially with a concentration of 50 mmol L^{-1} (peak I), then 70 mmol L^{-1} (peak II), the protein eluted at a concentration of 300 mmol L^{-1} (peak III) and finally 500 mmol L^{-1} (peak IV). The blue line represents the absorbance at 280 nm and the green line the concentration of Imidazole in the elution buffer.

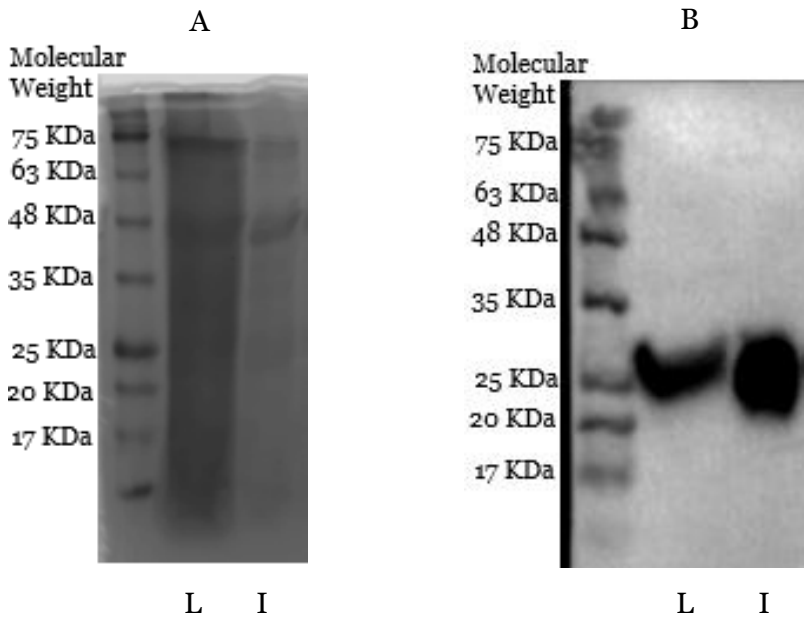

Figure 16 –SDS-PAGE analysis (A) and Western Bolt (B) of the SCOMT. Lane L – lysed SCOMT; I - Purified SCOMT from Peak III.

4.2 Studies for SCOMT stabilization

Recently, ionic liquids (ILs) have been considered as new biocompatible co-solvents for proteins [118]. Their uniquely tailored chemical and physical properties place ILs at the center of several protein-based applications such as crystallization, separation, extraction, solubilization and stabilization [119]. In this work, two major classes of ILs were studied. The first was choline-based IL, which has been extensively studied to reveal whether it promotes or inhibits protein aggregation and stabilization [120]. Second, imidazolium-based ILs such as [C_4mim]Cl have been employed as co-solvents or additives to suppress protein aggregation and promote protein refolding and crystallization [121]. Therefore, we evaluated the effect of the interaction of ionic liquids ([Ch][DHP] and [C_4mim]Cl]) in the enzymatic activity of SCOMT lysates, quantifying the amount of metanephrine formed by injecting the samples into HPLC by 12 hours. The corresponding metanephrine peak (elution time – 9 minutes and identified with an arrow in the chromatograms) was manually integrated and the peak value was used to calculate the SCOMT specific activity.

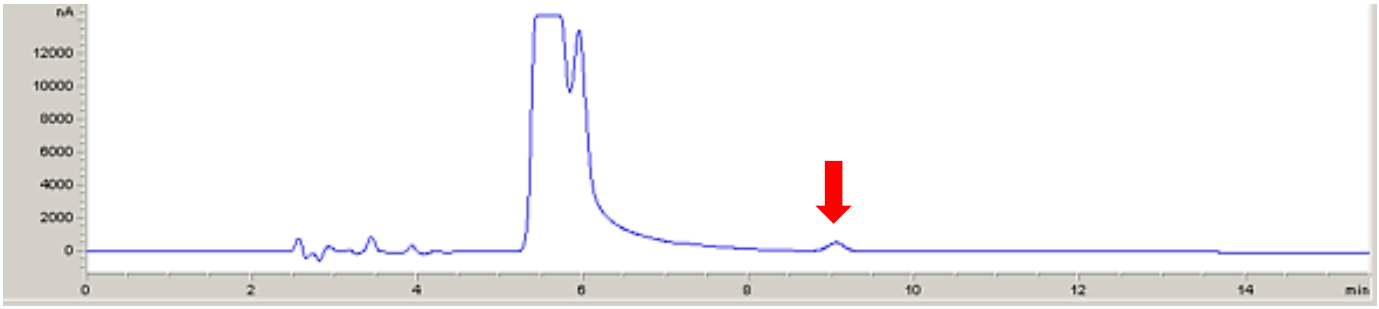

Figure 17 – SCOMT Lysate (Control) chromatogram at 4 °C where the sample consists of the SCOMT lysate in lysis buffer (150 mmol L^{-1} NaCl, 10 mmol L^{-1} DTT, 50 mmol L^{-1} Tris, 1 mmol L^{-1} $MgCl_2$, pH 8.0). Electrode 2 (reduction channel: - 350 mV).

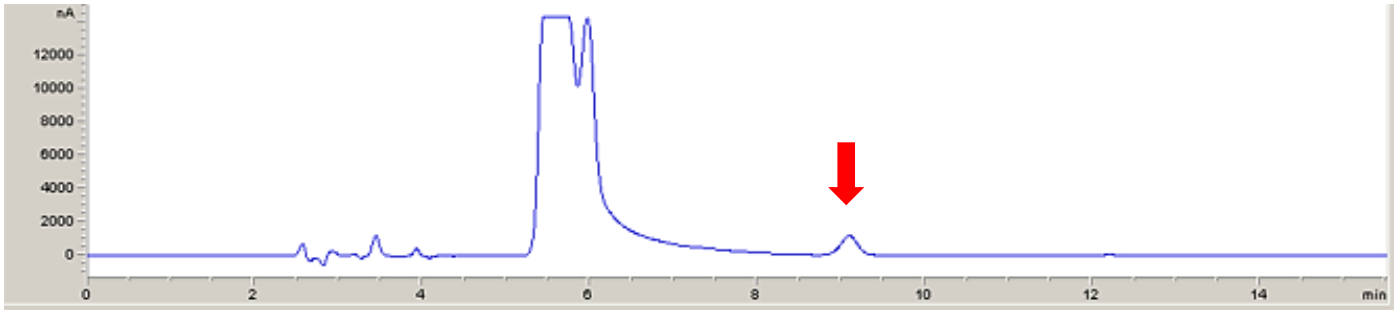

Figure 18 – SCOMT Lysate (Control) chromatogram at -80 °C where the sample consists of the SCOMT lysate in lysis buffer (150 mmol L^{-1} NaCl, 10 mmol L^{-1} DTT, 50 mmol L^{-1} Tris, 1 mmol L^{-1} $MgCl_2$, pH 8.0). Electrode 2 (reduction channel: - 350 mV).

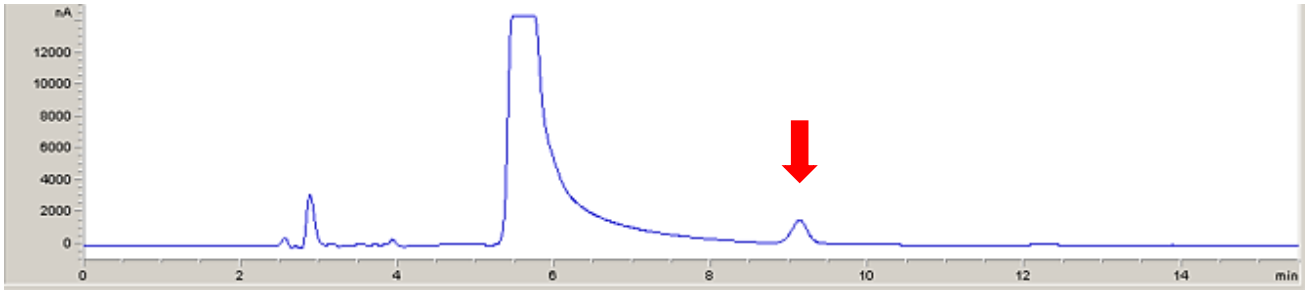

Figure 19 – Chromatogram of SCOMT lysate at 4 °C where the sample consists of SCOMT lysate in IL-free stabilizing buffer (5 mM trehalose, 15 mM cysteine, 5% glycerol, 150 mM NaCl, 1 mM $MgCl_2$ and 50 mM Tris pH= 7.8). Electrode 2 (reduction channel: - 350 mV).

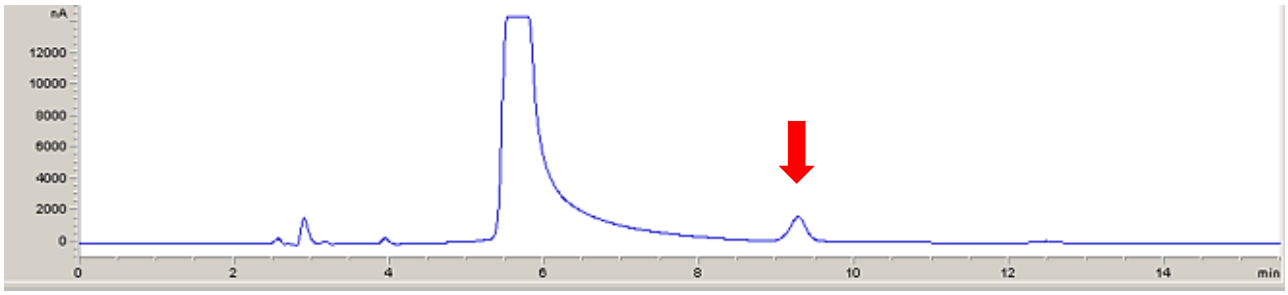

Figure 20 – Chromatogram of SCOMT lysate at 4 °C where the sample consists of SCOMT lysate in [C_4mim]Cl stabilizing buffer (5 mM trehalose, 15 mM cysteine, 5% glycerol, 150 mM NaCl, 1 mM $MgCl_2$, 50 mM Tris pH= 7.8 and 10 mM C_4minCl). Electrode 2 (reduction channel: - 350 mV).

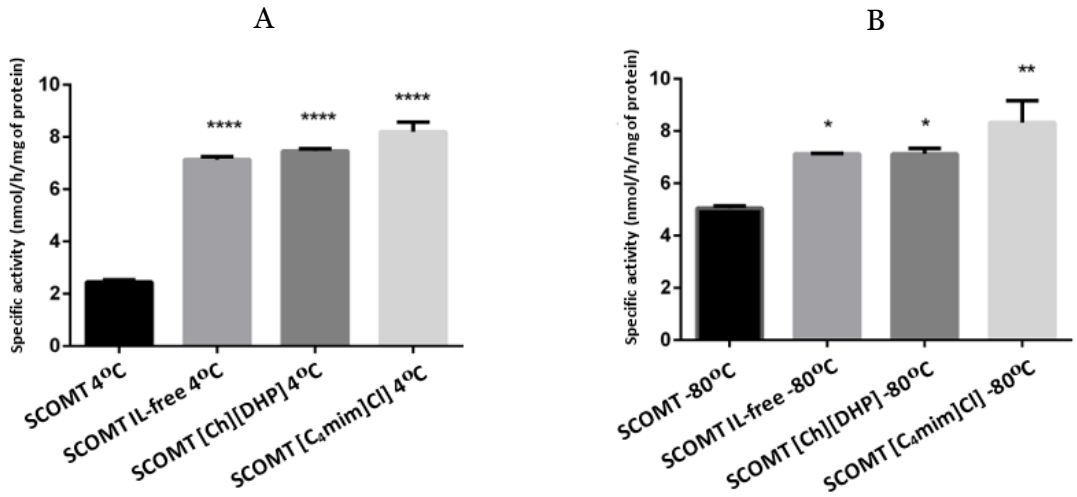

Figure 21 – SCOMT specific activity at 4 °C (A) and at -80 °C (B) after 12 hours of storage in distinct buffers (*p*-value * <0.05; ** <0.01; **** <0.0001).

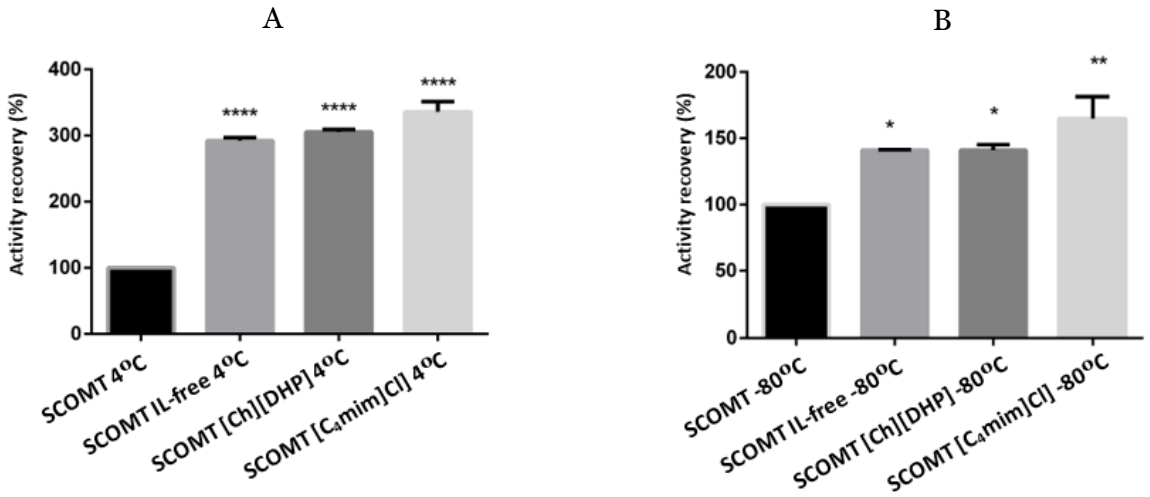

Figure 22 – SCOMT specific activity recovery at 4 ºC (A) and at -80 ºC (B) after 12 hours of storage in different buffers (*p*-value * <0.05; ** <0.01; **** <0.0001).

Once, during hSCOMTVal108-6His crystallization trials, the formation of cysteine crystals was observed when a concentration of 100 mM was used, lower concentrations of additives (15 mM cysteine, 5 mM trehalose, and 5% glycerol) were applied to stabilize the soluble enzyme as described for the membrane isoform hMBCOMTVal158 [40]. As previously mentioned, additives play an important role in protein stabilization. Namely, trehalose, protect proteins from denaturation *in vivo* and have also been described as promoters of protein folding and refolding [122]. Cysteines play a role in the formation of intramolecular and intermolecular disulfide bonds [123] that are essential to maintain the native three-dimensional structure. Finally, glycerol has been extensively applied for thermostabilization of enzymes [124] by mechanisms related to the exclusion of the solvophobic effect, which leads to protein conformations with a minimal surface area accessible to the solvent [38]. Then two distinct ILs classes, choline, with [Ch][DHP], and imidazole, with [C_4mim]Cl, were evaluated in hSCOMTVal108-6His lysates in terms of percentage of activity recovery at the two storage temperatures (4 °C and −80 °C), as shown in Figure 22. The addition of the mentioned additives, even at a low concentration, was able to maintain and even increase the percentage of hSCOMTVal108-6His activity recovery, with this increase being more significant at 4 °C. At -80 ºC, such significant results were not obtained and, by all indications, this behavior seems to be indicative of the phenomenon of cold denaturation, where a very low temperature leads to a decrease in the biological activity of hSCOMT [125,126]. As for the effect of the interaction of ILs on the enzymatic activity of the protein, it was observed that [C_4mim]Cl presents slightly better results than [Ch][DHP], in opposition to those observed for the membrane isoform [127]. Concerning p-values, the results were highly significant for the protein when stored at 4 °C for all the tested conditions (p-value < 0.0001), and significant when the protein was stored at −80 °C (p-value < 0.05 and p-value < 0.01).

4.3 Screening of SCOMT crystallization conditions

The main objective here was to screen the crystallization conditions of the purified SCOMT in a buffer containing 5 mM trehalose, 15 mM cysteine, 5% glycerol, 150 mM NaCl, 1 mM $MgCl_2$, 50 mM Tris pH= 7.8 and 10 mM [C_4min]Cl. Assays were carried out by Hanging Drop and Counter Diffusion methods (see sections 3.5.1 and 3.5.2, respectively) where several experimental conditions were investigated, more specifically, the composition of the protein solution, the precipitating agent and the temperature were changed. Afterwards, droplets and the capillaries were observed by optical microscopy and crystallization trials were classified. Further, the dye absorption test and the crush evaluation were carried out to assess if the crystals formed where from a protein or saline nature [128].

4.3.1 Temperature and precipitating agent

Temperature can be a significant parameter in the crystallization of biological macromolecules, and this often influences crystal nucleation and growth, affecting sample solubility and supersaturation. This is also relevant since we are limited to a restricted temperature range due to the characteristics of the protein[129]. The effect of temperature was tested to verify which one would lead to better results[129]. Crystallization trials were performed at a temperature of 4 ºC where the precipitating solution was composed of 0.1 M HEPES, pH=7.5 and 35% methyl-2,4-pentanediol and at a temperature of 20 ºC where the precipitating solution was composed of 0.1 M CAPS, 1.2 M NaH_2PO_4/0.8 M K_2HPO_4, pH= 10.5 and 0.2 M Li_2SO_4, as described in the literature [78]. In both assays the protein solution had an initial concentration of 2.72 mg protein/ml, but a real concentration of 1.36 mg/ml. Hanging drop and Counter diffusion methodologies are used to achieve a supersaturated solution and promote the crystal formation. With that in mind, we tested the influence of temperature given its influence on protein solubility.

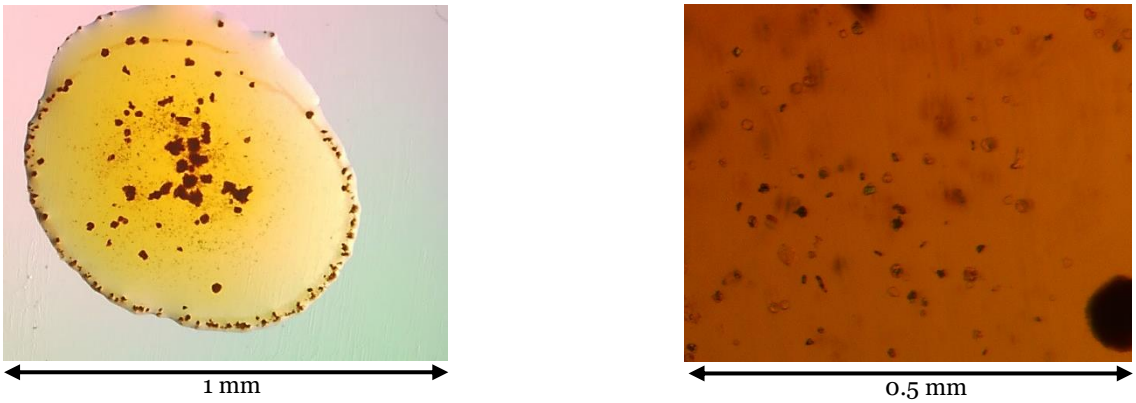

Figure 23 – Images captured 7 days after the Hanging Drop crystallization trials at 20 ºC. The drop shown is at 30x magnification and its close-up is at 80x magnification, where the final concentration of the reservoir solution is 0.05 M CAPS, 0.6 M NaH_2PO_4/0.4 M K_2HPO_4, pH= 10.5 and 0.1 M Li_2SO_4.

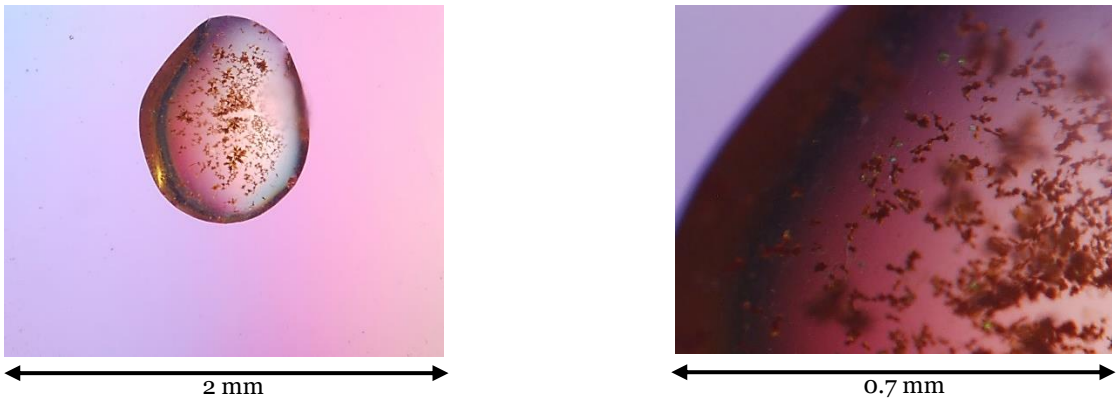

Figure 24 – Images captured 7 days after the Hanging Drop crystallization trials at 4 ºC. The drop shown is at 20x magnification and its close-up is at 70x magnification, where the final concentration of the reservoir solution is 0.05 M HEPES, pH=7.5 and 17.5% methyl-2,4-pentanediol.

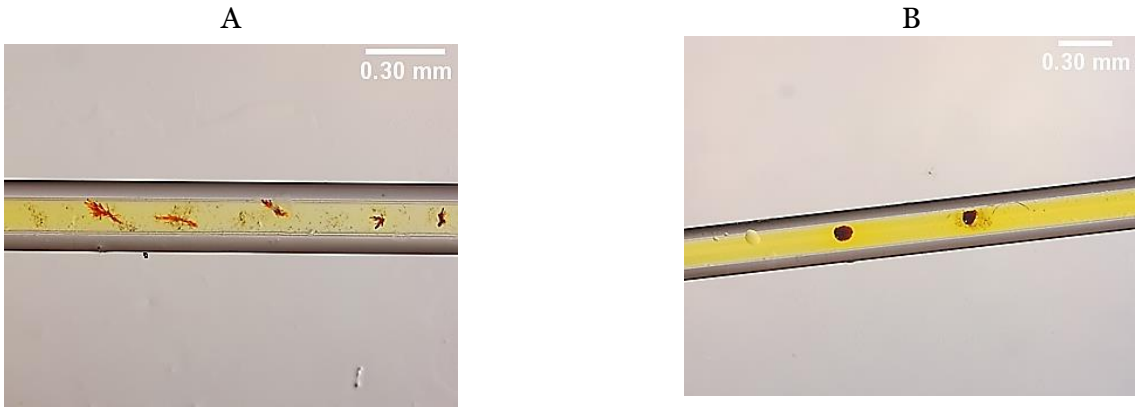

Figure 25 – Images captured 7 days after the Counter Diffusion crystallization trials at A-20 ºC and B-4 ºC. The capillaries were observed with a magnification of 30x and as a reference value, the capillary has a diameter of 0.30 mm.

Hanging-Drop results were observed 2 days after plate preparation and then every 5 days, while counter diffusion results, as it is a longer process, were observed every 7 days. The counter diffusion method is a more time-consuming process, as the supersaturation gradient is gradual, which allows the proteins to nucleate and undergo crystal growth in regions of lower supersaturation values, i.e., at the tip of the capillary closest to the salt , the supersaturation is higher, so we will have more small crystals and in greater numbers, while at the opposite end of the capillary we will have a lower supersaturation and, consequently, a smaller amount of larger crystals. As shown in the images, the crystallization assays at 4 ºC did not show promising results, therefore the crystallization tests carried out a posteriori were accomplished only at 20 ºC. At this temperature, it was possible to observe two types of crystals, needle-shaped and hexagonal-shaped. Those with a needle shape may be salt crystals and those with a hexagonal shape may be cysteine crystals, since it crystallizes easily [130]. Many precipitates are also observed in the drops, probably undissolved DNC, or salts present in the protein solution or in the precipitating solution. As DNC is slightly soluble in an aqueous buffer, it probably did not dissolve completely, which caused some precipitates.

This phenomenon occurred because, being a nonpolar compound, it has a low dielectric constant and makes it immiscible in water [131].

4.3.2 Concentration of the precipitating agent solution

As observed in section 4.3.1, in the various drops it is possible to observe a high number of precipitates. Since the precipitates observed may be salts present in the precipitant solution, crystallization tests were carried at different concentrations of precipitant and protein. The tests were carried out with proportions of the protein and precipitant solution of 1:1 and 2:1 (double the protein solution in relation to the precipitant solution) because, in this way, the volume of the precipitant solution is reduced to decrease the formation of precipitates. In both assays the protein solution had an initial concentration of 1.40 mg protein/ml, but real concentration of 0.70 mg/ml in the 1:1 ratio and 0.93 mg/ml in the 2:1 ratio.

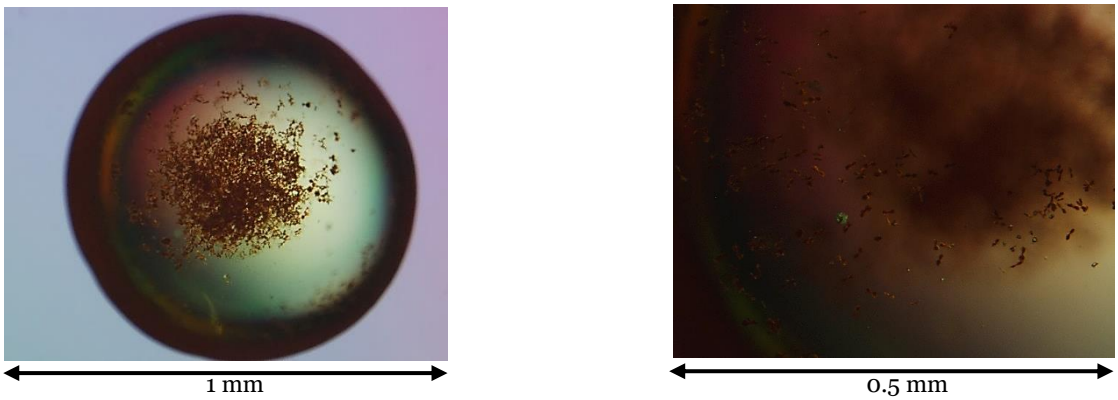

Figure 26 – Images captured 7 days after the Hanging drop test, where the 1:1 aspect ratio was tested. The drop shown is at 30x magnification and its close-up is at 80x magnification, where the final concentration of the reservoir solution is 0.05 M CAPS, 0.6 M NaH_2PO_4/0.4 M K_2HPO_4, pH= 10.5 and 0.1 M Li_2SO_4.

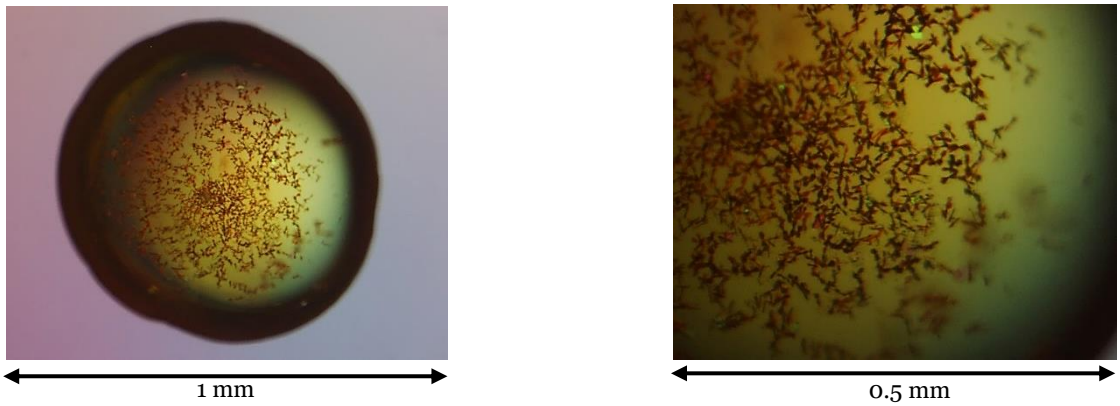

Figure 27 – Images captured 7 days after the Hanging drop test, where the 2:1 aspect ratio was tested. The drop shown is at 30x magnification and its close-up is at 80x magnification, where the final concentration of the reservoir solution is 0.03 M CAPS, 0.4 M NaH_2PO_4/0.27 M K_2HPO_4, pH= 10.5 and 0.07 M Li_2SO_4.

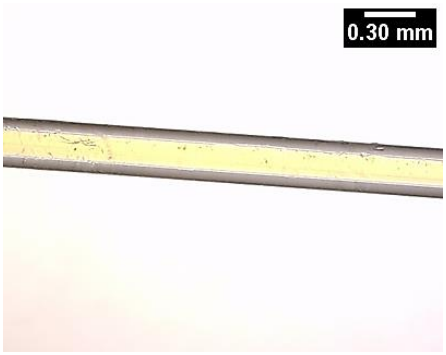

Figure 28 – Images captured 14 days after the Counter Diffusion test, where the initial concentration of the precipitating solution was reduced by half. The observed capillary has a magnification of 30x and as a reference value, the capillary has a diameter of 0.30 mm.

Hanging-Drop results were observed 2 days after plate preparation and then every 5 days, while counter diffusion results, as it is a longer process, were observed every 7 days. As the images suggest, although there is a significant number of precipitates in both cases, there appears to be a smaller number of precipitates and aggregates when decreasing the precipitant concentration. As described in the literature, the Counter Diffusion technique has as a criterion the fact that the protein concentration is between 4 mg/ml and 20 mg/ml, although a higher concentration can be used, and as in most of the tests carried out, the value concentration was less than 4 mg/ml, this was probably the predominant reason for the lack of results in the Counter Diffusion technique [132]. Since this technique was not showing positive results and to use the limiting volume of available protein more efficiently, only the hanging drop technique was performed.

4.3.3 Influence of SAM and DNC

In the following crystallization trials, it was study whether the presence of SAM and DNC would influence the crystallization process, using only the hanging drop technique. Due to the difficulty of diluting the DNC in the protein solution as verified in the previous tests, it was also tested if we could dilute the DNC in dimethyl sulfoxide (DMSO) to verify if we would observe a smaller number of precipitates in the drop. DMSO at relatively low concentrations can alter the properties of proteins in solution, leading to protein denaturation, aggregation, and degradation [133]. Thus, to dissolve DNC in DMSO, we used a higher concentration of DNC and dissolved it in 100 mL of DMSO. Since DMSO at a concentration above 5% (v/v) is toxic for proteins, we dilute the stock solution to have the desired DNC concentration (50 mM) and respect the 5% (v/v) concentration of DMSO. The tests were carried out with the precipitating solution composed of 0.1 M CAPS, 1.2 M NaH_2PO_4/0.8 M K_2HPO_4, pH= 10.5 and 0.2 M Li_2SO_4 and with the initial protein concentration of 4.4 mg protein/ml and real concentration of 2.2 mg/ml.

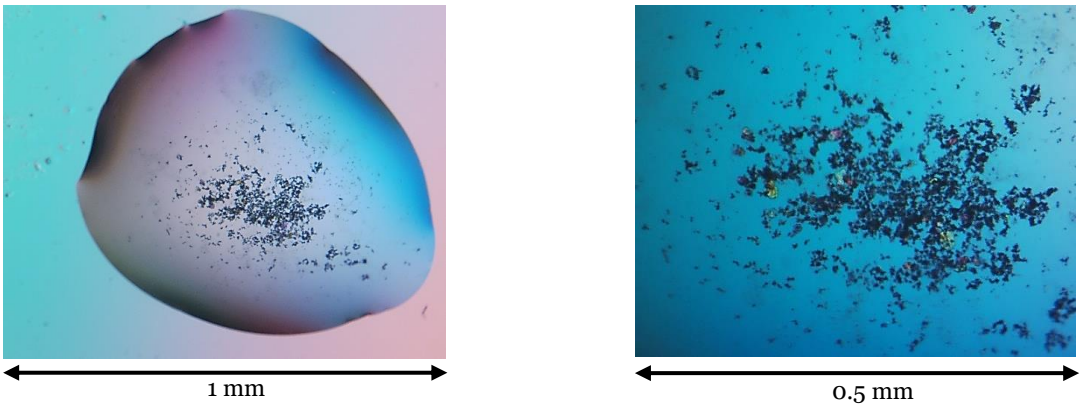

Figure 29 – Image captured 7 days after the start of the hanging drop test experiments, where only SCOMT is present. The drop shown is at 30x magnification and its close-up is at 80x magnification, where the final concentration of the reservoir solution is 0.05 M CAPS, 0.6 M NaH_2PO_4/0.4 M K_2HPO_4, pH= 10.5 and 0.1 M Li_2SO_4.

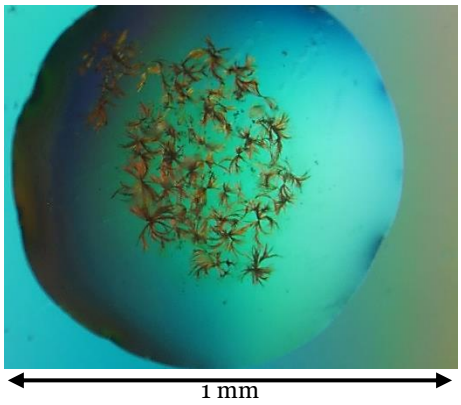

Figure 30 – Image captured 7 days after the start of the hanging drop test experiments, where SCOMT+DNC. The drop shown is at 30x magnification, where the final concentration of the reservoir solution is 0.05 M CAPS, 0.6 M NaH_2PO_4/0.4 M K_2HPO_4, pH= 10.5 and 0.1 M Li_2SO_4 + 25 mM DNC.

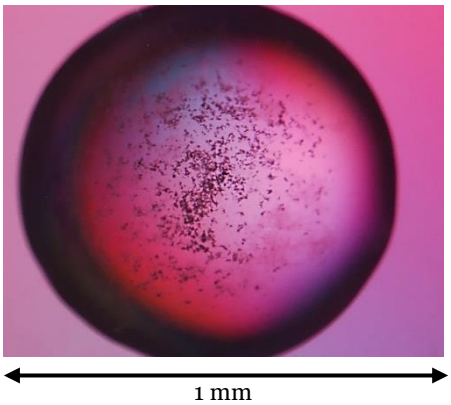

Figure 31 – Image captured 7 days after the start of the hanging drop test experiments, where SCOMT+SAM. The drop shown is at 30x magnification, where the final concentration of the reservoir solution is 0.05 M CAPS, 0.6 M NaH_2PO_4/0.4 M K_2HPO_4, pH= 10.5 and 0.1 M Li_2SO_4 + 25 mM SAM.

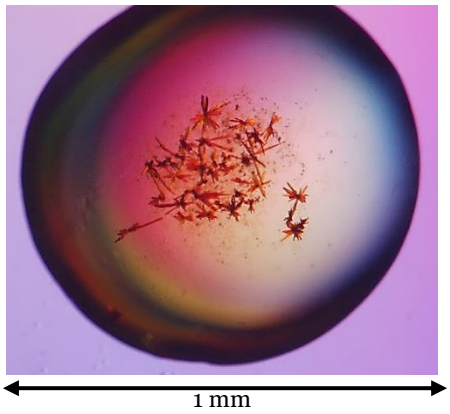

Figure 32 – Image captured 7 days after the start of the hanging drop test experiments, where SCOMT+SAM+DNC. The drop shown is at 30x magnification, where the final concentration of the reservoir solution is 0.05 M CAPS, 0.6 M NaH_2PO_4/0.4 M K_2HPO_4, pH= 10.5 and 0.1 M Li_2SO_4 + 25 mM SAM + 25 mM DNC.

Hanging-Drop results were observed 2 days after plate preparation and every 5 days thereafter. A precipitate is something more amorphous that does not have a well-defined shape, whereas a crystal is a solid with a well-defined shape [134]. But this observation becomes difficult given the magnification used and the size of the solids that were formed. Sometimes it appears to be a precipitate, but when we increase magnification, we realize that they are very small crystals. Thus, in the crystallization trials carried out with the presence of DNC, the presence of orange precipitates is observed, which suggests that some of the precipitates are DNC , that is, the method used to dissolve the inhibitor has to be optimized. Precipitates are also observed in drops that do not contain DNC, which are probably precipitates of salts present in the precipitant solution such as NaH_2PO_4, K_2HPO_4 and Li_2SO_4 or precipitates of compounds present in the protein solution, as is the case of cysteine. Unfortunately, it was not clear whether both SAM and DNC are essential to crystallize SCOMT, as the crystals that are observed in the images are flat hexagonal plates, typical morphology of cysteine crystals [130] . In general, when DNC is present, it seems that we have less precipitates, that is, we have precipitates of an orange hue that appear to be the inhibitor, but the remaining precipitates, which could be salts, seem to be in smaller quantities when compared to assays without DNC.

4.3.4 Dye absorption test

Because protein molecules are large and irregularly shaped, they are often not compacted optimally [135]. This leads to channels and cavities in the crystal lattice that are large enough to accommodate dye molecules. Salt crystals, however, are usually packed in such a way as to occlude all solvent, or usually anything much larger than a water molecule. So, if the crystals are the same color as the dye itself, they must be protein crystals. Therefore, this test was done to try to distinguish salt crystals from protein crystals using 2 dyes, Thymol

Blue and Coomassie Blue. The trials were carried out with the precipitating solution composed of 0.1 M CAPS, 1.2 M NaH_2PO_4/0.8 M K_2HPO_4, pH= 10.5 and 0.2 M Li_2SO_4 and with the initial protein concentration of 4.4 mg protein/ml and real concentration of 2.2 mg/ml.

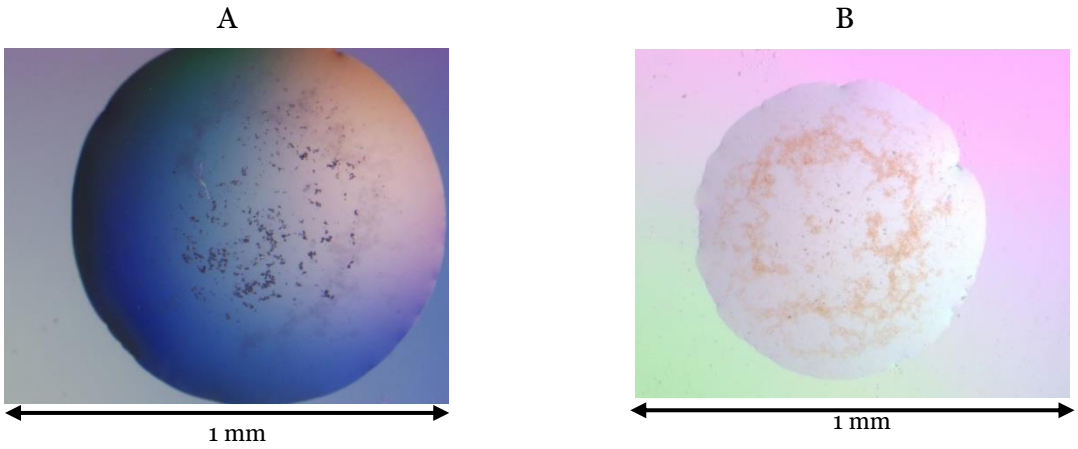

Figure 33 – Images captured 7 days after the hanging drop crystallization trials, where only SCOMT is present with A- Thymol blue and B- Coomassie blue. The drops shown have a magnification of 30x, where the final concentration of the reservoir solution is 0.05 M CAPS, 0.6 M NaH_2PO_4/0.4 M K_2HPO_4, pH= 10.5 and 0.1 M Li_2SO_4 and the final protein concentration is 2.2 mg/ml.

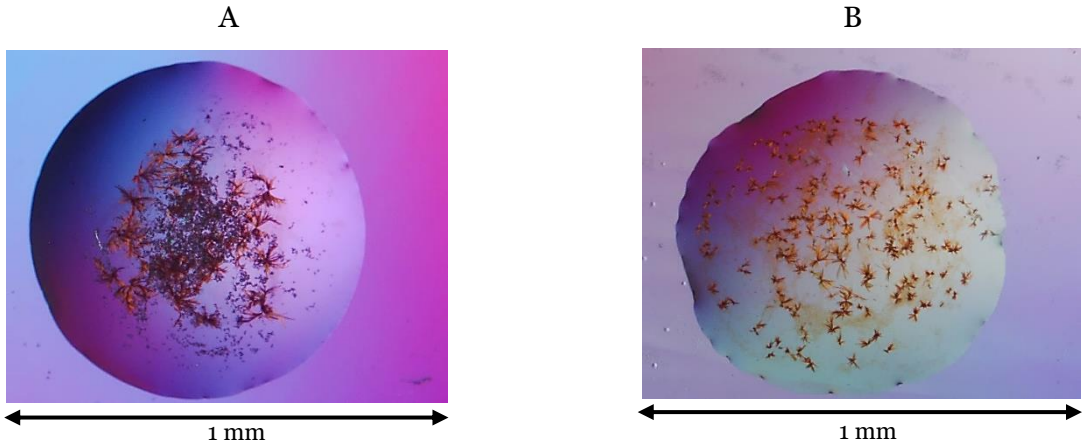

Figure 34 – Images captured 7 days after the hanging drop test, where SCOMT+DNC is present with A- Thymol blue and B- Coomassie blue. The drops shown have a magnification of 30x, where the final concentration of the reservoir solution is 0.05 M CAPS, 0.6 M NaH_2PO_4/0.4 M K_2HPO_4, pH= 10.5 and 0.1 M Li_2SO_4 and the final protein concentration is 2.2 mg/ml + 25 mM DNC.

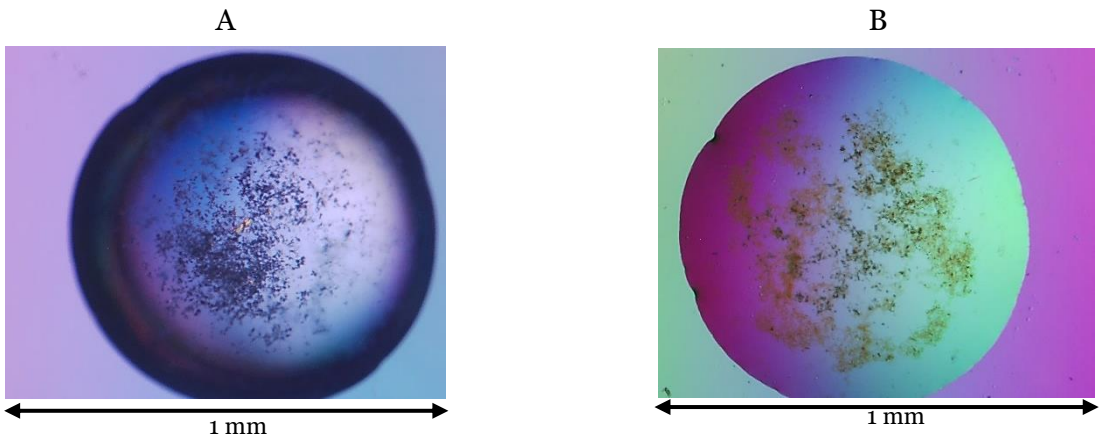

Figure 35 – Images captured 7 days after the hanging drop test, where SCOMT+SAM is present with A- Thymol blue and B- Coomassie blue. The drops shown have a magnification of 30x, where the final concentration of the reservoir solution is 0.05 M CAPS, 0.6 M NaH_2PO_4/0.4 M K_2HPO_4, pH= 10.5 and 0.1 M Li_2SO_4 and the final protein concentration is 2.2 mg/ml + 25 mM SAM.

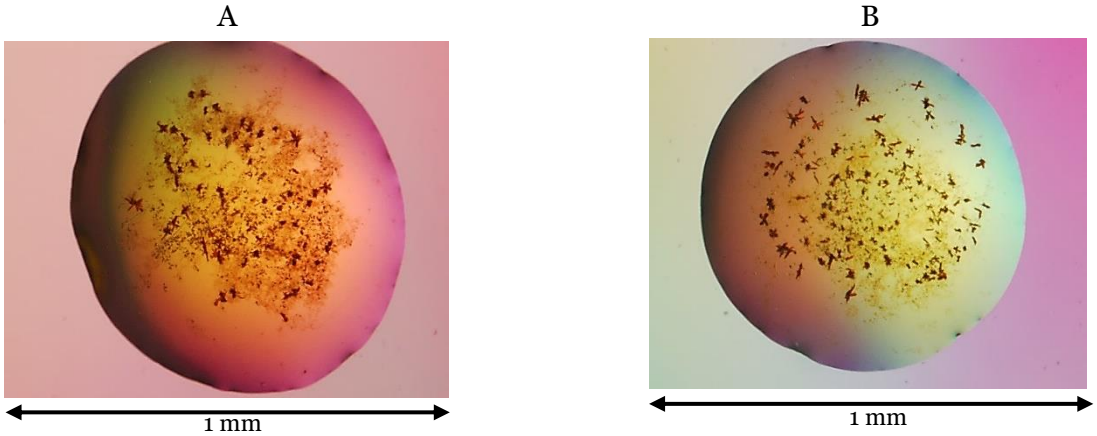

Figure 36 – Images captured 7 days after the hanging drop test, where SCOMT+SAM+DNC is present with A- Thymol blue and B- Coomassie blue. The drops shown have a magnification of 30x, where the final concentration of the reservoir solution is 0.05 M CAPS, 0.6 M NaH_2PO_4/0.4 M K_2HPO_4, pH= 10.5 and 0.1 M Li_2SO_4 and the final protein concentration is 2.2 mg/ml + 25 mM SAM + 25 mM DNC.

Hanging-Drop results were observed 2 days after plate preparation and every 5 days thereafter. The dyes did not show conclusive results, as none of the crystals stood out. This probably happened because no protein crystals were formed. The resulting images have a different color due to a feature of the optical microscope that diffracts light and thus is used to distinguish precipitates from crystals. In some images it is evident that there are "brighter" crystals that can be salt crystals.

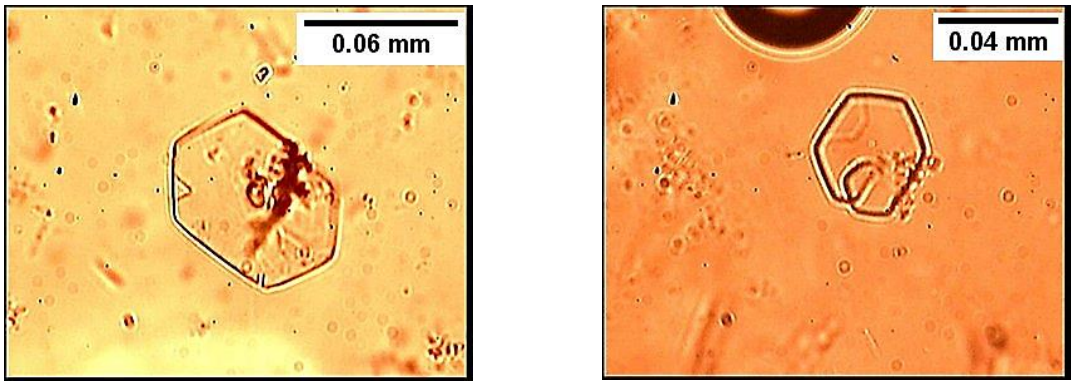

Figure 37 – Microscopic images of the crystals obtained at x10 and x40 magnification and with a size, respectively, of about 0.06 mm and 0.04 mm.

Several crystals were observed during the crystallization trials but due to their small size it was difficult to perform tests that enable to highlight protein crystals characteristics and namely distinguish them from salt crystals. Most seem to be cysteine crystals comparing them with the crystals obtained in the literature as they have a similarity in their shape, a hexagonal shape [130].

Experimental tests were performed, and several approaches were considered to identify the protein crystals. Initially, the strategy would be to identify the crystals by X-rays, but due to their small size, the idea was discarded since for diffraction analysis and due to the equipment available at the Instituto de Investigação e Inovação em Saúde (i3S), the protein crystals needed be at least 0.1 mm in the longest dimension, to provide a sufficient volume of crystal lattice that can be exposed to the beam [136]. As an alternative, the crush test was performed, which consisted of pressing the crystal manually with the aid of a kind of glass rod and if it broke easily, it is a protein crystal but due to the small size of the crystals, it was impossible to "hunt" just one crystal to perform this technique. Finally, dye absorption tests were performed, but no stained crystals were observed, i.e., either no protein crystals were present, or the dye solution was not sufficiently stained to exert the effect its function.

Chapter 5 – Conclusions

Nowadays, given the physiological relevance of COMT in the *O*-methylation of catecholamines and catechol estrogens, as well as the number of diseases associated with this enzyme, COMT is seen as a therapeutic target of a high clinical impact. Obtaining protein crystals is important to support structural biology investigations. Thus, it is relevant to have protein crystal structures as it will have many applications such as medicinal chemistry through structural biology, protein-based drug development, scale-up, separation and purification, drug formulation and application. In this work, we studied the influence of ionic liquids on the stability of the SCOMT lysate and investigated its crystallization conditions. First, we studied the influence of two ionic liquids (ILs), [Ch][DHP] and [C_4mim]Cl, on the stability of SCOMT present in crude lysates for 12 hours at temperatures of 4 ºC and -80 ºC and whether ILs would increase the specific activity of the protein, so, in relation to temperature, the one that presented the best results in terms of activity was at 4 ºC in the presence of C_4mimCl (an increase of about 350 % in relation to the control sample without stabilization buffer). At this stage, it was concluded that the best temperature to maintain the stability of the protein would be 4 ºC and that the use of ILs, more specifically [C_4mim]Cl, would be an asset to increase the stability and activity of SCOMT during the storage. Then, crystallization tests were carried out using two methodologies, Hanging Drop and Counter-Diffusion, where temperature, protein concentration, concentration and type of solution of the precipitating agent and the influence of SAM and DNC were evaluated. At one point, the Counter-Diffusion method was abolished as it did not show positive results and to use the limiting volume of available protein more efficiently, only the Hanging Drop technique was performed. In this sense, we obtained a greater number of crystals at 20 ºC, but the variation in the concentration of the precipitating agent solution did not present a significant improvement on the main results. Regarding the influence of SAM and DNC, unfortunately it was not possible to perceive whether both SAM and DNC are essential to crystallize SCOMT, but it allowed identifying the nature of some precipitates, such as DNC or salts present in the reservoir solution, and the nature of the crystals , more specifically, cysteine crystals. The next step was the attempt to distinguish the protein crystals from the salt crystals, but due to their small size, it was not possible to identify with certainty their nature, although several tests were carried out, such as the absorption of dyes (Timol Blue and Coomassie) and the crush test.

In conclusion, regarding the future perspectives, the use of [C_4mim]Cl is an asset in the stability of SCOMT as verified in the results and the next step will be to obtain crystals of this protein to facilitate and start the inhibition studies of this isoform. To overcome the main difficulties encountered in this study, regarding the issue of DNC, the preparation of a more concentrated solution of DNC in DMSO should be investigated. As for the solution of the precipitating agent, other concentrations than those used should be tested or look for

another type of precipitating agent to obtain clearer drops and thus facilitate the task of classifying the experimental results.

Chapter 6 – References

1. Usman A, Lobb K, Pletschke BI, Whiteley CG, Wilhelmi BS. Interaction of silver nanoparticles with catechol O-methyltransferase: Spectroscopic and simulation analyses. *Biochem Biophys Rep*. 2021;26. doi:10.1016/j.bbrep.2021.101013

2. Axelrod J, Tomchick R. *Enzymatic o-Methylation of Epinephrine and Other Catechols**.

3. Myöhänen TT, Männistö PT. Distribution and functions of catechol-O-methyltransferase proteins. Do recent findings change the picture? In: *International Review of Neurobiology*. Vol 95. Academic Press Inc.; 2010:29-47. doi:10.1016/B978-0-12-381326-8.00003-X

4. Kiss LE, Soares-Da-Silva P. Medicinal chemistry of catechol O -methyltransferase (COMT) inhibitors and their therapeutic utility. *J Med Chem*. 2014;57(21):8692-8717. doi:10.1021/jm500572b

5. Wang FY, Wang P, Zhao DF, et al. Analytical methodologies for sensing catechol-O-methyltransferase activity and their applications. *J Pharm Anal*. 2021;11(1):15-27. doi:10.1016/j.jpha.2020.03.012

6. Bastos P, Gomes T, Ribeiro L. Catechol-O-methyltransferase (COMT): An update on its role in cancer, neurological and cardiovascular diseases. In: *Reviews of Physiology, Biochemistry and Pharmacology*. Vol 173. Springer Verlag; 2017:1-39. doi:10.1007/112_2017_2

7. Lin C hsien. P1‐264: CATECHOL‐O‐METHYLTRANSFERASE (*COMT*) GENETIC VARIANTS ARE ASSOCIATED WITH COGNITIVE DECLINE IN PATIENTS WITH PARKINSON'S DISEASE. Published online 2018:382-383.

8. Chang CC. Catechol-O-methyltransferase Val158Met polymorphism on structural covariance networks in Alzheimer's disease. *J Neurol Sci*. 2017;381(2017):321. doi:10.1016/j.jns.2017.08.909

9. Wang H, Zhang B, Zeng B, et al. Association between catechol-O-methyltransferase genetic variation and functional connectivity in patients with first-episode schizophrenia. *Schizophr Res*. 2018;199:214-220. doi:10.1016/j.schres.2018.04.023

10. Robinson RG, Smith SM, Wolkenberg SE, et al. Characterization of non-nitrocatechol pan and isoform specific catechol-O-methyltransferase inhibitors and substrates. *ACS Chem Neurosci*. 2012;3(2):129-140. doi:10.1021/cn200109w

11. Bai HW, Shim JY, Yu J, Bao TZ. Biochemical and molecular modeling studies of the O-methylation of various endogenous and exogenous catechol substrates catalyzed by recombinant human soluble and membrane-bound catechol-O-methyltransferases. *Chem Res Toxicol*. 2007;20(10):1409-1425. doi:10.1021/tx700174w

12. Wardle MC, Hart AB, Palmer AA, de Wit H. Does COMT genotype influence the effects of d-amphetamine on executive functioning? *Genes Brain Behav*. 2013;12(1):13-20. doi:10.1111/gbb.12012

13. Chen J, Song J, Yuan P, et al. Orientation and cellular distribution of membrane-bound catechol-O-methyltransferase in cortical neurons: Implications for drug development. *Journal of Biological Chemistry*. 2011;286(40):34752-34760. doi:10.1074/jbc.M111.262790

14. Ellingson T, Duddempudi S, Greenberg BD, Hooper D, Eisenhofer G. Determination of differential activities of soluble and membrane-bound catechol-O-methyltransferase in tissues and erythrocytes. *J Chromatogr B Biomed Sci Appl*. 1999;729(1-2):347-353. doi:10.1016/S0378-4347(99)00125-5

15. Mannisto PT, Ulmanen I, Lundstrom K, et al. Characteristics of catechol O-methyltransferase (COMT) and properties of selective COMT inhibitors. *Progress in Drug Research*. 1992;39:291-350. doi:10.1007/978-3-0348-7144-0_9

16. Zhu BT, Conney AH. Functional role of estrogen metabolism in target cells: Review and perspectives. *Carcinogenesis*. 1998;19(1):1-27. doi:10.1093/carcin/19.1.1

17. Vidgren J, Tilgmann C, MelCn K, Julkunen I, Taskinentn J. *Kinetics of Human Soluble and Membrane-Bound Catechol o-Methyltransferase: A Revised Mechanism and Description of the Thermolabile Variant of the Enzyme*. Vol 34.; 1995.

18. Vieira-Coelho MA, Soares-Da-Silva P. *Effects of Tolcapone upon Soluble and Membrane-Bound Brain and Liver Catechol-O-Methyltransferase*. Vol 821.; 1999.

19. Lachman HM, Papolos DF, Saito T, Yu YM, Szumlanski CL, Weinshilboum RM. Human catechol-O-methyltransferase pharmacogenetics: Description of a functional polymorphism and its potential application to neuropsychiatric disorders. *Pharmacogenetics*. 1996;6(3):243-250. doi:10.1097/00008571-199606000-00007

20. Wedrén S, Rudqvist TR, Granath F, et al. Catechol-O-methyltransferase gene polymorphism and post-menopausal breast cancer risk. *Carcinogenesis*. 2003;24(4):681-687. doi:10.1093/carcin/bgg022

21. Karayiorgou M, Altemus M, Galke BL, et al. Genotype determining low catechol-O-methyltransferase activity as a risk factor for obsessive-compulsive disorder. *Proc Natl Acad Sci U S A*. 1997;94(9):4572-4575. doi:10.1073/pnas.94.9.4572

22. Karen A. Nolan, Jan. Volavka, Pa`l Czobor, et al. Suicidal behavior in patients with schizophrenia is related to COMT polymorphism. Accessed July 5, 2022. https://doi.org/10.1097/00041444-200010030-00003

23. Zubieta JK, Heitzeg MM, Smith YR, et al. COMT val158 genotype affects μ-opioid neurotransmitter responses to a pain stressor. *Science (1979)*. 2003;299(5610):1240-1243. doi:10.1126/science.1078546

24. Hosák L. Role of the COMT gene Val158Met polymorphism in mental disorders: A review. *European Psychiatry*. 2007;22(5):276-281. doi:10.1016/j.eurpsy.2007.02.002

25. Acquas E, Carboni E, Ree RHA de, da Prada M, Chiara G di, Roche HL. *Extracellular Concentrations of Dopamine and Metabolites in the Rat Caudate After Oral Administration of a Novel Catechol-o-Methyltransferase Inhibitor Ro 40-7592*.

26. Muellner J, Gharrad I, Habert MO, et al. Dopaminergic denervation severity depends on COMT Val158Met polymorphism in Parkinson's disease. *Parkinsonism Relat Disord*. 2015;21(5):471-476. doi:10.1016/j.parkreldis.2015.02.009

27. Lee SG, Joo Y, Kim B, et al. Association of Ala72Ser polymorphism with COMT enzyme activity and the risk of schizophrenia in Koreans. *Hum Genet*. 2005;116(4):319-328. doi:10.1007/s00439-004-1239-y

28. Fekete S, Veuthey JL, Guillarme D. New trends in reversed-phase liquid chromatographic separations of therapeutic peptides and proteins: Theory and applications. *J Pharm Biomed Anal*. 2012;69:9-27. doi:10.1016/j.jpba.2012.03.024

29. Yu A, Shibata Y, Shah B, Calamini B, Lo DC, Morimoto RI. Protein aggregation can inhibit clathrin-mediated endocytosis by chaperone competition. *Proc Natl Acad Sci U S A*. 2014;111(15). doi:10.1073/pnas.1321811111

30. Ciryam P, Kundra R, Morimoto RI, Dobson CM, Vendruscolo M. Supersaturation is a major driving force for protein aggregation in neurodegenerative diseases. *Trends Pharmacol Sci*. 2015;36(2):72-77. doi:10.1016/j.tips.2014.12.004

31. Pedro AQ, Oppolzer D, Bonifácio MJ, Maia CJ, Queiroz JA, Passarinha LA. Evaluation of MutS and Mut+ Pichia pastoris Strains for Membrane-Bound Catechol-O-Methyltransferase Biosynthesis. *Appl Biochem Biotechnol*. 2015;175(8):3840-3855. doi:10.1007/s12010-015-1551-0

32. Yang L, Yan J, Deng Y. Purification and identification of soluble Catechol-O-methyltransferase from rat liver. *2010 4th International Conference on Bioinformatics and Biomedical Engineering, iCBBE 2010*. Published online 2010:25-28. doi:10.1109/ICBBE.2010.5517422

33. Pihlavisto P, Reenila I. Separation methods for catechol O-methyltransferase activity assay: Physiological and pathophysiological relevance. *J Chromatogr B Analyt Technol Biomed Life Sci*. 2002;781(1-2):359-372. doi:10.1016/S1570-0232(02)00429-4

34. Cotton NJH, Stoddard B, Parson WW. Oxidative inhibition of human soluble catechol-o-methyltransferase. *Journal of Biological Chemistry*. 2004;279(22):23710-23718. doi:10.1074/jbc.M401086200

35. Mukalel AJ, Evans BC, Kilchrist K v., et al. Excipients for the lyoprotection of MAPKAP kinase 2 inhibitory peptide nano-polyplexes. *Journal of Controlled Release*. 2018;282(April):110-119. doi:10.1016/j.jconrel.2018.04.045

36. Ajito S, Iwase H, Takata SI, Hirai M. Sugar-Mediated Stabilization of Protein against Chemical or Thermal Denaturation. *Journal of Physical Chemistry B*. 2018;122(37):8685-8697. doi:10.1021/acs.jpcb.8b06572

37. Knape MJ, Ballez M, Burghardt NC, et al. Divalent metal ions control activity and inhibition of protein kinases. *Metallomics*. 2017;9(11):1576-1584. doi:10.1039/c7mt00204a

38. Vagenende V, Yap MGS, Trout BL. Mechanisms of protein stabilization and prevention of protein aggregation by glycerol. *Biochemistry*. 2009;48(46):11084-11096. doi:10.1021/bi900649t

39. Bozorgmehr MR, Monhemi H. How can a free amino acid stabilize a protein? insights from molecular dynamics simulation. *J Solution Chem*. 2015;44(1):45-53. doi:10.1007/s10953-015-0291-7

40. Gonçalves AM, Sousa Â, Pedro AQ, et al. Advances in Membrane-Bound Catechol-O-Methyltransferase Stability Achieved Using a New Ionic Liquid-Based Storage Formulation. *Int J Mol Sci*. 2022;23(13). doi:10.3390/ijms23137264

41. Gomes D, Gonçalves C, Gonçalves AM, Queiroz JA, Sousa A, Passarinha LA. Applications of gellan natural polymer microspheres in recombinant catechol-O-methyltransferase direct capture from a Komagataella pastoris lysate. *Int J Biol Macromol*. 2021;172:186-196. doi:10.1016/j.ijbiomac.2020.12.225

42. Ma Z, Liu H, Wu B. Structure-based drug design of catechol-O-methyltransferase inhibitors for CNS disorders. *Br J Clin Pharmacol*. 2014;77(3):410-420. doi:10.1111/bcp.12169

43. Passarinha LA, Bonifácio MJ, Soares-da-Silva P, Queiroz JA. A new approach on the purification of recombinant human soluble catechol-O-methyltransferase from an Escherichia coli extract using hydrophobic interaction chromatography. *J Chromatogr A*. 2008;1177(2):287-296. doi:10.1016/j.chroma.2007.06.002

44. Czarnota S, Johannissen LO, Baxter NJ, et al. Equatorial Active Site Compaction and Electrostatic Reorganization in Catechol- O-methyltransferase. *ACS Catal*. 2019;9(5):4394-4401. doi:10.1021/acscatal.9b00174

45. Espírito Santo GM, Pedro AQ, Oppolzer D, et al. Development of fed-batch profiles for efficient biosynthesis of catechol-O-methyltransferase. *Biotechnology Reports*. 2014;3:34-41. doi:10.1016/j.btre.2014.05.005

46. Gao L, Fang JS, Bai XY, et al. In silico target fishing for the potential targets and molecular mechanisms of baicalein as an antiparkinsonian agent: Discovery of the protective effects on nmda receptor-mediated neurotoxicity. *Chem Biol Drug Des*. 2013;81(6):675-687. doi:10.1111/cbdd.12127

47. Haasio K. Toxicology and safety of comt inhibitors. In: *International Review of Neurobiology*. Vol 95. Academic Press Inc.; 2010:163-189. doi:10.1016/B978-0-12-381326-8.00007-7

48. Ericsson AD. Potentiation of the l-Dopa effect in man by the use of catechol-O-methyltransferase inhibitors. *J Neurol Sci*. 1971;14(2):193-197. doi:10.1016/0022-510X(71)90088-8

49. Bonifácio MJ, Palma PN, Almeida L, Soares-Da-Silva P. *Catechol-O-Methyltransferase and Its Inhibitors in Parkinson's Disease*. Vol 13. Blackwell Publishing Inc; 2007.

50. Moschovou K, Melagraki G, Mavromoustakos T, Zacharia LC, Afantitis A. Cheminformatics and virtual screening studies of COMT inhibitors as potential

Parkinson's disease therapeutics. *Expert Opin Drug Discov*. 2020;15(1):53-62. doi:10.1080/17460441.2020.1691165

51. Cacabelos R. Parkinson's disease: From pathogenesis to pharmacogenomics. *Int J Mol Sci*. 2017;18(3). doi:10.3390/ijms18030551

52. Polak PE, Lin SX, Pelligrino D, Feinstein DL. The blood-brain barrier-permeable catechol-O-methyltransferase inhibitor dinitrocatechol suppresses experimental autoimmune encephalomyelitis. *J Neuroimmunol*. 2014;276(1-2):135-141. doi:10.1016/j.jneuroim.2014.09.004

53. Salamon A, Zádori D, Szpisjak L, Klivényi P, Vécsei L. Opicapone for the treatment of Parkinson's disease: an update. *Expert Opin Pharmacother*. 2019;20(18):2201-2207. doi:10.1080/14656566.2019.1681971

54. Schultz E, Nissinen E. Inhibition of rat liver and duodenum soluble catechol-O-methyltransferase by a tight-binding inhibitor OR-462. *Biochem Pharmacol*. 1989;38(22):3953-3956. doi:10.1016/0006-2952(89)90673-4

55. Backstrom R, Honkanen E, Pippuri A, et al. *Synthesis of Some Novel Potent and Selective Catechol o -Methyltransferase Inhibitors*. Vol 32.; 1989.

56. Nissinen E, Linden IB, Schultz E, Kaakkola S, M~innist~ PT, Pohto P. *Inhibition of Catechoi-O-Methyitransferase Activity by Two Novel Disubstituted Catechols in the Rat*. Vol 153.; 1988.

57. Borgulya J, Bruderer H, Bernauer K, Ziircher G, da Prada M. *04. Catechol-o-Methyltransferase-Inhibiting Pyrocatechol Derivatives: Synthesis and Structure-Activity Studies*. Vol 72.; 1989.

58. Castro Caldas A, Teodoro T, Ferreira JJ. The launch of opicapone for Parkinson's disease: negatives versus positives. *Expert Opin Drug Saf*. 2018;17(3):331-337. doi:10.1080/14740338.2018.1433659

59. Jiménez-Luna J, Pérez-Benito L, Martínez-Rosell G, et al. DeltaDelta neural networks for lead optimization of small molecule potency. *Chem Sci*. 2019;10(47):10911-10918. doi:10.1039/c9sc04606b

60. Bonifácio MJ, Loureiro AI, Torrão L, et al. Species differences in pharmacokinetic and pharmacodynamic properties of nebicapone. *Biochem Pharmacol*. 2009;78(8):1043-1051. doi:10.1016/j.bcp.2009.05.036

61. Palma PN, Rodrigues ML, Archer M, et al. Comparative study of ortho- and meta-nitrated inhibitors of catechol-O-methyltransferase: Interactions with the active site and regioselectivity of O-methylation. *Mol Pharmacol*. 2006;70(1):143-153. doi:10.1124/mol.106.023119

62. Palma PN. Mechanisms of pharmacoresistance in epilepsy View project BIA 2-093 View project. doi:10.13140/2.1.1292.3848

63. Greenwood J, Pham H, Rey J. Opicapone: A third generation COMT inhibitor. *Clin Park Relat Disord*. 2021;4(November 2020):100083. doi:10.1016/j.prdoa.2020.100083

64. Reichmann H, Lees A, Magalhães D, Rocha J, Soares-Da-Silva P. Opicapone in clinical practice in Parkinson's disease German patients with motor fluctuations: Findings from the OPTIPARK study. *J Neurol Sci*. 2021;429(2021):119429. doi:10.1016/j.jns.2021.119429

65. Greenwood J, Pham H, Rey J. Opicapone: A third generation COMT inhibitor. *Clin Park Relat Disord*. 2021;4. doi:10.1016/j.prdoa.2020.100083

66. Bonifácio MJ, Sutcliffe JS, Torrão L, Wright LC, Soares-Da-Silva P. Brain and peripheral pharmacokinetics of levodopa in the cynomolgus monkey following administration of opicapone, a third generation nitrocatechol COMT inhibitor. *Neuropharmacology*. 2014;77:334-341. doi:10.1016/j.neuropharm.2013.10.014

67. Bicker J, Alves G, Fortuna A, Soares-Da-Silva P, Falcão A. A new PAMPA model using an in-house brain lipid extract for screening the blood-brain barrier permeability of drug candidates. *Int J Pharm*. 2016;501(1-2):102-111. doi:10.1016/j.ijpharm.2016.01.074

68. Chai Z, Fan HJ, Li YR, et al. Effect of Wuzi Yanzong Pill on oxidative stress response in Parkinson's disease mice. *J Neurol Sci*. 2019;405:29. doi:10.1016/j.jns.2019.10.265

69. Fabbri M, Ferreira JJ, Lees A, et al. Opicapone for the treatment of Parkinson's disease: A review of a new licensed medicine. *Movement Disorders*. 2018;33(10):1528-1539. doi:10.1002/mds.27475

70. Malherbe P, Bertocci B, Caspers P, Zürcher G, da Prada M. Expression of Functional Membrane-Bound and Soluble Catechol-O-Methyltransferase in Escherichia coli and a Mammalian Cell Line. *J Neurochem*. 1992;58(5):1782-1789. doi:10.1111/j.1471-4159.1992.tb10054.x

71. Vogl T, Hartner FS, Glieder A. New opportunities by synthetic biology for biopharmaceutical production in Pichia pastoris. *Curr Opin Biotechnol*. 2013;24(6):1094-1101. doi:10.1016/j.copbio.2013.02.024

72. Cregg JM, Cereghino JL, Shi J, Higgins DR. *Recombinant Protein Expression 23 MOLECULAR BIOTECHNOLOGY REVIEW 23 Recombinant Protein Expression in Pichia Pastoris*.; 2000. www.kgi.edu/html/

73. Espírito Santo GM, Pedro AQ, Oppolzer D, et al. Development of fed-batch profiles for efficient biosynthesis of catechol-O-methyltransferase. *Biotechnology Reports*. 2014;3:34-41. doi:10.1016/j.btre.2014.05.005

74. Junge F, Schneider B, Reckel S, Schwarz D, Dötsch V, Bernhard F. Large-scale production of functional membrane proteins. *Cellular and Molecular Life Sciences*. 2008;65(11):1729-1755. doi:10.1007/s00018-008-8067-5

75. Pedro AQ, Correia FF, Santos FM, et al. Biosynthesis and purification of histidine-tagged human soluble catechol-O-methyltransferase. *Journal of Chemical Technology and Biotechnology*. 2016;91(12):3035-3044. doi:10.1002/jctb.4930

76. Lundström K, Tilgmann C, Peränen J, Kalkkinen N, Ulmanen I. Expression of enzymatically active rat liver and human placental catechol-O-methyltransferase in Escherichia coli; purification and partial characterization of the enzyme. *BBA - Gene Structure and Expression*. 1992;1129(2):149-154. doi:10.1016/0167-4781(92)90479-J

77. Tilgmann C, Ulmanen I. Purification methods of mammalian catechol-O-methyltransferase. *J Chromatogr B Biomed Appl*. 1996;684(1-2):147-161. doi:10.1016/0378-4347(96)00117-X

78. Rutherford K, le Trong I, Stenkamp RE, Parson WW. Crystal Structures of Human 108V and 108M Catechol O-Methyltransferase. *J Mol Biol*. 2008;380(1):120-130. doi:10.1016/j.jmb.2008.04.040

79. Passarinha LA, Bonifácio MJ, Queiroz JA. ORIGINAL RESEARCH Comparative study on the interaction of recombinant human soluble catechol-O-methyltransferase on some hydrophobic adsorbents. *Biomed Chromatogr*. 2007;21:430-438. doi:10.1002/bmc

80. Mooney JT, Fredericks DP, Zhang C, et al. Purification of a recombinant human growth hormone by an integrated IMAC procedure. *Protein Expr Purif*. 2014;94:85-94. doi:10.1016/j.pep.2013.11.002

81. Boden V, Winzerling JJ, Vijayalakshmi M, Porath J. Rapid one-step purification of goat immunoglobulins by immobilized metal ion affinity chromatography. *J Immunol Methods*. 1995;181(2):225-232. doi:10.1016/0022-1759(95)00006-V

82. Skarka A, Škarydová L, Štambergová H, Wsól V. Purification and reconstitution of human membrane-bound DHRS7 (SDR34C1) from Sf9 cells. *Protein Expr Purif*. 2014;95:44-49. doi:10.1016/j.pep.2013.11.013

83. Fanou-Ayi L, Vijayalakshmi M. *Metal-Chela Te Affinity Chroma Tograph y as a Separation Tool*.

84. Cheung RCF, Wong JH, Ng TB. Immobilized metal ion affinity chromatography: A review on its applications. *Appl Microbiol Biotechnol*. 2012;96(6):1411-1420. doi:10.1007/s00253-012-4507-0

85. Vekilov PG. The two-step mechanism of nucleation of crystals in solution. *Nanoscale*. 2010;2(11):2346-2357. doi:10.1039/c0nr00628a

86. McPherson A, Gavira JA. Introduction to protein crystallization. *Acta Crystallographica Section F:Structural Biology Communications*. 2014;70(1):2-20. doi:10.1107/S2053230X13033141

87. Rupp B. Origin and use of crystallization phase diagrams. *Acta Crystallogr F Struct Biol Commun*. 2015;71:247-260. doi:10.1107/S2053230X1500374X

88. Dessau MA, Modis Y. Protein crystallization for X-ray crystallography. *Journal of Visualized Experiments*. 2010;(47). doi:10.3791/2285

89. Patel S, Cudney Bob, Alex Mcpherson. Polymeric Precipitants for the Crystallization of Macromolecules. *University of California, Riverside, Department of Biochemistry, Riverside, CA 92521*. 1995;207(2):819-828.

90. Englard S, Seifter S. *[22] PRECIPITATION TECHNIQUES 285 [22] Precipitation Techniques*.; 1990.

91. Cohn J, Hughes L, Weare J. Preparation and Proporties of Serum and Plasma Proteins. *Department of Physical Chemistry,Harvard Medical School*. 1947;69:1753-1761.

92. Garside J. *Nucleation*.

93. Caserta G. *Chemical Maturation of Hydrogenases : An Insight into Artificial and Biohybrid Systems*.; 2018. https://tel.archives-ouvertes.fr/tel-01631276

94. Goulart DB. Principles of lactose crystallization and rheology of milk protein concentrate. *Research, Society and Development*. 2021;10(15):e577101523028. doi:10.33448/rsd-v10i15.23028

95. Melia TP, Moffitt WP. *CRYSTALLIZATION FROM AQUEOUS SOLUTION*. Vol 19.; 1964.

96. Li D, Liu S, Wei Y, Ren T, Tang Y. A turbulent two-phase model for predicting cavitating flow based on homogenous nucleation theory. *International Communications in Heat and Mass Transfer*. 2018;97:17-29. doi:10.1016/j.icheatmasstransfer.2018.06.001

97. Celik FA, Yildiz AK. Molecular dynamics simulation of crystallization kinetics and homogenous nucleation of Pt-Rh alloy. *J Non Cryst Solids*. 2015;415:36-41. doi:10.1016/j.jnoncrysol.2015.02.011

98. Erdemir D, Lee AY, Myerson AS. Nucleation of crystals from solution: Classical and two-step models. *Acc Chem Res*. 2009;42(5):621-629. doi:10.1021/ar800217x

99. *3.2.1. Fundamentals of Homogeneous Nucleation*.

100. Gebauer D. How can additives control the early stages of mineralisation? *Minerals*. 2018;8(5). doi:10.3390/min8050179

101. *The Handbook of Continuous Crystallization*. Royal Society of Chemistry; 2020. doi:10.1039/9781788013581

102. Thakore SD, Sood A, Bansal AK. Emerging role of primary heterogeneous nucleation in pharmaceutical crystallization. *Drug Dev Res*. 2020;81(1):3-22. doi:10.1002/ddr.21622

103. Pichlo C, Montada AA, Schacherl M, Baumann U. Production, crystallization and structure determination of C. Difficile PPEP-1 via microseeding and zinc-SAD. *Journal of Visualized Experiments*. 2016;2016(118). doi:10.3791/55022

104. McPherson A, Kuznetsov YG, Malkin A, Plomp M. Macromolecular crystal growth as revealed by atomic force microscopy. *J Struct Biol*. 2003;142(1):32-46. doi:10.1016/S1047-8477(03)00036-4

105. *Sitting Drop Vapor Diffusion Crystallization*.; 1991.

106. Growth C. *Plates for Hanging Drop Vapor Diffusion 24 Well, Use 22 Mm Cover Slide HR3-140 VDX™ Plate without Sealant-100 Plate Case HR3-170 VDX™ Plate with Sealant-100 Plate Case Sealing Grease HR3-510 Dow Corning ® Vacuum Grease,*

150 Gram Tube-Each HR3-508 Dow Corning ® 7 Release Compound Grease, 150 Gram Tube-Each Other Items for Hanging Drop Vapor Diffusion HR4-430 Sticky Pad-Each Hanging Drop Vapor Diffusion Crystallization.

107. *Diaplate for Microdialysis Crystallization*.

108. Ehler A, Benz J, Schlatter D, Rudolph MG. Mapping the conformational space accessible to catechol-O-methyltransferase. *Acta Crystallogr D Biol Crystallogr*. 2014;70(8):2163-2174. doi:10.1107/S1399004714012917

109. Ellermann M, Paulini R, Jakob-Roetne R, et al. Molecular recognition at the active site of catechol-O-methyltransferase (COMT): Adenine replacements in bisubstrate inhibitors. *Chemistry - A European Journal*. 2011;17(23):6369-6381. doi:10.1002/chem.201003648

110. Lerner C, Jakob-Roetne R, Buettelmann B, Ehler A, Rudolph M, Sarmiento RMR. Design of Potent and Druglike Nonphenolic Inhibitors for Catechol O-Methyltransferase Derived from a Fragment Screening Approach Targeting the S-Adenosyl- l -methionine Pocket. *J Med Chem*. 2016;59(22):10163-10175. doi:10.1021/acs.jmedchem.6b00927

111. Ellermann M, Lerner C, Burgy G, et al. Catechol-O-methyltransferase in complex with substituted 3´-deoxyribose bisubstrate inhibitors. *Acta Crystallogr D Biol Crystallogr*. 2012;68(3):253-260. doi:10.1107/S0907444912001138

112. Harrison ST, Poslusney MS, Mulhearn JJ, et al. Synthesis and evaluation of heterocyclic catechol mimics as inhibitors of catechol-o-methyltransferase (COMT). *ACS Med Chem Lett*. 2015;6(3):318-323. doi:10.1021/ml500502d

113. Gallardo E P la. An Improved HPLC Method for Quantification of Metanephrine with Coulometric Detection. *J Chromatogr Sep Tech*. 2014;05(02). doi:10.4172/2157-7064.1000217

114. Correia FF, Santos FM, Pedro AQ, Bonifácio MJ, Queiroz JA, Passarinha LAP. Recovery of biological active catechol-O-methyltransferase isoforms from Q-sepharose. *J Sep Sci*. 2014;37(1-2):20-29. doi:10.1002/jssc.201300977

115. Learmonth DA, Palma PN, Vieira-Coelho MA, Soares-Da-Silva P. Synthesis, biological evaluation, and molecular modeling studies of a novel, peripherally selective inhibitor of catechol-O-methyltransferase. *J Med Chem*. 2004;47(25):6207-6217. doi:10.1021/jm0408480

116. Garcia-Ruiz JM. *User Guide HR3-194 (Page 1) How to Use the GCB-By*.

117. Fazen CH, Kahkoska AR, Doyle RP. Expression and purification of human PYY(3-36) in Escherichia coli using a His-tagged small ubiquitin-like modifier fusion. *Protein Expr Purif*. 2012;85(1):51-59. doi:10.1016/j.pep.2012.06.015

118. Fujita K. Ionic Liquids as Stabilization and Refolding Additives and Solvents for Proteins. In: *Advances in Biochemical Engineering/Biotechnology*. Vol 168. Springer Science and Business Media Deutschland GmbH; 2019:215-226. doi:10.1007/10_2018_65

119. Cintolo-Gonzalez JA, Braun D, Blackford AL, et al. Breast cancer risk models: a comprehensive overview of existing models, validation, and clinical applications. *Breast Cancer Res Treat*. 2017;164(2):263-284. doi:10.1007/s10549-017-4247-z

120. Reslan M, Ranganathan V, Macfarlane DR, Kayser V. Choline ionic liquid enhances the stability of Herceptin® (trastuzumab). *Chemical Communications*. 2018;54(75):10622-10625. doi:10.1039/c8cc06397d

121. Pusey ML, Paley MS, Turner MB, Rogers RD. Protein crystallization using room temperature ionic liquids. *Cryst Growth Des*. 2007;7(4):787-793. doi:10.1021/cg060696t

122. Leibly DJ, Nguyen TN, Kao LT, Hewitt SN, Barrett LK, van Voorhis WC. Stabilizing Additives Added during Cell Lysis Aid in the Solubilization of Recombinant Proteins. *PLoS One*. 2012;7(12). doi:10.1371/journal.pone.0052482

123. Liu T, Wang Y, Luo X, et al. Enhancing protein stability with extended disulfide bonds. *Proc Natl Acad Sci U S A*. 2016;113(21):5910-5915. doi:10.1073/pnas.1605363113

124. Castro GR. *Properties of Soluble-Chymotrypsin in Neat Glycerol and Water*.; 2000. www.elsevier.com/locate/enzmictec

125. Sanfelice D, Temussi PA. Cold denaturation as a tool to measure protein stability. *Biophys Chem*. 2016;208:4-8. doi:10.1016/j.bpc.2015.05.007

126. Siddiqui KS, Cavicchioli R. Cold-adapted enzymes. *Annu Rev Biochem*. 2006;75:403-433. doi:10.1146/annurev.biochem.75.103004.142723

127. Chen Q, Hui R, Sun C, Gu X, Luo M, Zheng X. Soluble expression, purification, and stabilization of a pro-apoptotic human protein, CARP. *Protein Expr Purif*. 2006;45(2):329-334. doi:10.1016/j.pep.2005.07.011

128. *Salt or Protein Crystals?*

129. *Temperature as a Crystallization Variable*.

130. Rimer JD, An Z, Zhu Z, et al. Crystal growth inhibitors for the prevention of L-cystine kidney stones through molecular design. *Science (1979)*. 2010;330(6002):337-341. doi:10.1126/science.1191968

131. Galamba N, Paiva A, Barreiros S, Simões P. Solubility of Polar and Nonpolar Aromatic Molecules in Subcritical Water: The Role of the Dielectric Constant. *J Chem Theory Comput*. 2019;15(11):6277-6293. doi:10.1021/acs.jctc.9b00505

132. Otálora F, Gavira JA, Ng JD, García-Ruiz JM. Counterdiffusion methods applied to protein crystallization. *Prog Biophys Mol Biol*. 2009;101(1-3):26-37. doi:10.1016/j.pbiomolbio.2009.12.004

133. Tjernberg A, Markova N, Griffiths WJ, Hallén D. DMSO-related effects in protein characterization. *J Biomol Screen*. 2006;11(2):131-137. doi:10.1177/1087057105284218

134. Crystalline and Amorphous Solids.

135. Weichenberger CX, Afonine P v., Kantardjieff K, Rupp B. The solvent component of macromolecular crystals. *Acta Crystallogr D Biol Crystallogr*. 2015;71:1023-1038. doi:10.1107/S1399004715006045

136. Smyth MS, Martin JHJ. *Review x Ray Crystallography*. Vol 53.; 2000.